

ON THE DEVELOPMENT OF THE ANGIOTENSIN IV LIGANDS,  
NORLEUAL AND NLE<sup>1</sup>-ANGIOTENSIN IV, AS ANTI-CANCER  
AND WOUND HEALING AGENTS

By

PATRICK DAVID ELIAS

A dissertation submitted in partial fulfillment of  
the requirements for the degree of

DOCTOR OF PHILOSOPHY

WASHINGTON STATE UNIVERSITY  
Graduate Program in Pharmacology/Toxicology

August 2008

© Copyright by PATRICK DAVID ELIAS, 2008  
All Rights Reserved



To the Faculty of Washington State University:

The members of the Committee appointed to examine the dissertation/thesis of PATRICK DAVID ELIAS find it satisfactory and recommend that it be accepted.

---

Chair

---

---

---

---

---

## ACKNOWLEDGMENT

I would like to thank my mentor, Dr. Joseph Harding, for guidance and support throughout my graduate training at Washington State University. Dr. Harding's support and advice has been invaluable and I will treasure it throughout my personal and professional life.

I would also like to thank the additional members of my thesis committee including Dr. Jay Wright, Dr. Michael Varnum, Dr. Barb Sorg, and Dr. Raymond Quock for their professional support and advice during my training.

Thank you to my colleagues and friends, Dr. Brent Yamamoto, Bryan Hudson, Alene McCoy, and Drs. Pete and Starla Meighan for their helpful advice and lab support.

I would also like to recognize my parents, brothers, sister, and father and mother-in-law, for their love and support throughout this endeavor.

Lastly, but most importantly, I would like to thank my beautiful wife and daughter, Becky and Daphne, for putting up with this insanity and believing in my dream. Without your love and support I would not be where I am today.

ON THE DEVELOPMENT OF THE ANGIOTENSIN IV LIGANDS,  
NORLEUAL AND NLE<sup>1</sup>-ANGIOTENSIN IV, AS ANTI-CANCER  
AND WOUND HEALING AGENTS

Abstract

By Patrick David Elias, Ph.D.  
Washington State University  
August 2008

Chair: Joseph W. Harding

Cancer and defective wound healing continue to be formidable clinical challenges accounting for billions of dollars in health care expenditures annually. Newly emerging treatment modalities for treating these diseases include the design and recombinant production of growth factors to promote wound healing and monoclonal antibodies to inhibit primary and secondary tumor development. These therapies have shown to be effective, but expensive to produce. In this dissertation, we provide an alternative to recombinant technology in the form of peptide agonists and antagonists. These molecules are relatively inexpensive and simple to synthesize with potent affinities for their target sites.

In this dissertation, we show that the AT<sub>4</sub> antagonist, Norleual, blocks c-Met signaling and cellular effects in Madin-Darby Canine Kidney cells, providing further evidence to support its anti-cancer mechanism of action. In addition, we show that an AT<sub>4</sub> agonist, Nle<sup>1</sup>-AngIV, accelerates both normal and impaired wound healing.

## TABLE OF CONTENTS

	Page
ACKNOWLEDGEMENTS.....	iii
ABSTRACT.....	iv
LIST OF FIGURES.....	vii
CHAPTER	
1. INTRODUCTION.....	1
The Renin-Angiotensin System.....	1
The AT <sub>4</sub> Receptor System.....	1
AT <sub>4</sub> Receptor System Anti-Cancer Mechanism of Action.....	3
The HGF/c-Met Receptor System.....	4
MDCK Cells: The Classical Cellular Model for c-Met Activity.....	6
Wound Healing.....	7
Impaired Wound Healing.....	9
Matrix Metalloproteinases (MMPs).....	10
References.....	12
2. THE ANGIOTENSIN IV LIGAND, NORLEUAL, INHIBITS HEPATOCTE GROWTH FACTOR (HGF)/C-MET STIMULATED CELLULAR PHENOMENA VIA THE C-MET-UROKINASE PLASMINOGEN ACTIVATOR (UPA) SIGNALING PATHWAY.....	17
Summary.....	17
Introduction.....	18
Materials and Methods.....	20

Results & Discussion.....	24
Acknowledgements.....	29
References.....	30
Figure Legends.....	34
Figures.....	36
3. THE ANGIOTENSIN IV LIGAND, NLE <sup>1</sup> -ANGIOTENSIN IV (NLE <sup>1</sup> -ANG IV), ACCELERATES DERMAL WOUND REPAIR.....	40
Abstract.....	40
Introduction.....	40
Methods.....	42
Results.....	48
Discussion.....	54
Acknowledgements.....	57
References.....	58
Figure Legends.....	61
Figures.....	65
4. CONCLUSION.....	71
Figure Legends.....	74
Figures.....	75

## LIST OF FIGURES

1. NORLEUAL COMPETES WITH HGF FOR BINDING AND DISRUPTS C-MET ACTIVATION AND DOWNSTREAM SIGNALING IN HEK 293 CELLS.....	3
2. NORLEUAL ATTENUATES HGF/C-MET PROLIFERATION.....	36
3. NORLEUAL INHIBITS MDCK CELL INVASION AND MIGRATION.....	36
4. NORLEUAL INHIBITS MDCK CELL SCATTERING.....	37
5. NORLEUAL BLOCKS ERK ACTIVATION BY HGF/C-MET.....	38
6. NORLEUAL PERTURBS HGF/C-MET UPA INDUCTION.....	39
7. NLE <sup>1</sup> -ANGIV STIMULATES HFF PROLIFERATION, MIGRATION, AND WOUND HEALING.....	65
8. NLE <sup>1</sup> -ANGIV STIMULATES PHOSPHORYLATED-ERK IN HFFS.....	67
9. NLE <sup>1</sup> -ANGIV INHIBITS EXCISIONAL WOUND DEHISCENCE.....	67
10. SYSTEMIC NLE <sup>1</sup> -ANGIV TREATMENT CAUSES EARLY SCAB RELEASE AND INCREASES THE BREAKING STRENGTH OF INCISIONAL WOUNDS.....	68
11. NLE <sup>1</sup> -ANGIV INCREASES WOUND COLLAGEN DEPOSITION.....	69
12. NLE <sup>1</sup> -ANGIV DECREASES INCISIONAL WOUND DEHISCENCE.....	70
13. NLE <sup>1</sup> -ANGIV ATTENUATES MMP-2 ACTIVITY.....	70
14. NLE <sup>1</sup> -ANGIV AND DERIVATIVES STIMULATE PROLIFERATION.....	75
15. NORLEUAL-6AH AND ANALOGS ATTENUATE C-MET MIGRATION.....	75



For Becky and Daphne

## Chapter I

### Introduction

#### Part I

#### ***The Renin-Angiotensin System***

The renin-angiotensin system (RAS) mediates many classical physiological processes including body-water balance, blood pressure regulation, cyclicity of reproductive hormones, and sexual behaviors. The RAS involves mainly three receptor subtypes ( $AT_1$ ,  $AT_2$ , and  $AT_4$ ) that have a broad tissue distribution and regulate a vast array of physiologies. The endogenous production of multiple ligands is accomplished through a series of enzymatic steps that convert inactive angiotensinogen to produce the AngI, AngII, AngIII, and AngIV ligands. Angiotensin converting enzyme cleaves AngI to generate the AngII receptor ligand, which is cleaved on the N-terminus by aminopeptidase A to produce the heptapeptide, AngIII. AngIII is a substrate for aminopeptidase N, which cleaves AngIII on the N-terminus to generate AngIV. AngIV goes through further processing by aminopeptidases and carboxypeptidases to produce inactive dipeptides. The  $AT_1$  receptor, which binds AngII and AngIII, mediates the classical physiologies of the RAS. AngIV has a distinct high-affinity binding site, which regulates renal and cerebral blood flow, angiogenesis, and learning and memory (Wright et. al., 2004, Progress in Neuro & Handa et. al. 1999, J Pharm Exp Ther).

#### ***The $AT_4$ Receptor System***

The hexapeptide that is generated by enzymatic catalysis from AngIII was originally thought to be biologically inactive for two reasons (Zhang et. al., 1998, J Pharm Exp Ther & Briand S et. al., 1999, J Cell Biochem). First, AngIV demonstrates a poor affinity for the AT<sub>1</sub> and AT<sub>2</sub> receptor. Second, the AngII and AngIII peptides were superior to the AngIV peptides at eliciting angiotensin-dependent effects (Wright et. al., 2004, Progress in Neuro). However, in 1993 our lab discovered a distinct receptor that could bind these peptides reversibly and with high affinity. Using autoradiography, we discovered a distinct receptor now known as the AT<sub>4</sub> receptor, which demonstrates a broad tissue distribution. It is found in high density in the adrenals, bladder, colon, heart, kidney, prostate, and central nervous system. Several sites in the central nervous system demonstrated a high density of AngIV binding, including the hippocampus, neocortex, and cerebellum. Since then, our lab has synthesized over four hundred peptides and peptidomimetics which bind reversibly and with high affinity to this site and elicit dramatic effects on learning and memory consolidation. We have identified a number of our molecules as AT<sub>4</sub> receptor agonists based on their ability to facilitate learning in the Morris Water Maze task. Conversely, there are several molecules in this family that we have identified as antagonists based on their ability to block learning and memory in this model.

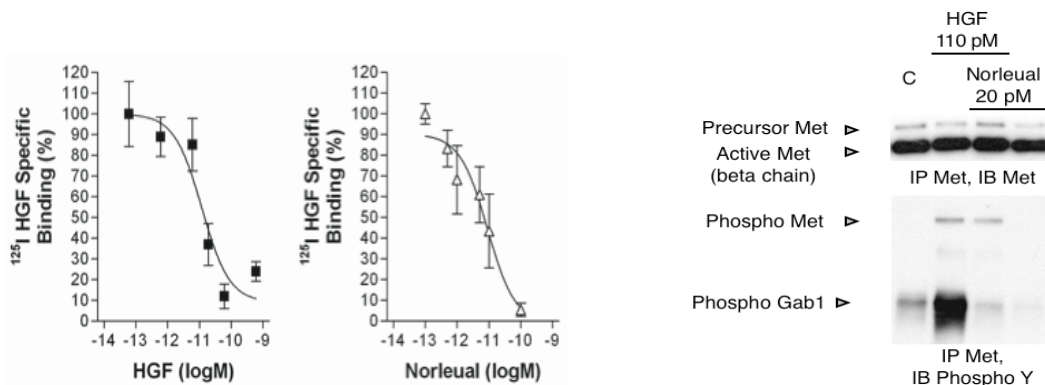
With the discovery of agonists and antagonists and the numerous tissues that they were discovered to bind to came the idea that these molecules may have therapeutic potential. The finding that there was a relatively high density of AngIV binding on the aortic endothelial cells of the heart suggested that AT<sub>4</sub>

ligands may be able to influence the angiogenic process and have anti-cancer activity. Subsequent to this finding, numerous studies have shown that the AT<sub>4</sub> antagonist, Norleual, blocks primary tumor growth, tumor angiogenesis, and metastases.

### ***The AT<sub>4</sub> Receptor System Anti-Cancer Mechanism of Action***

The molecular identity of the AT<sub>4</sub> receptor system has recently been elucidated. Using Norleual, our laboratory discovered that Norleual competes with Hepatocyte Growth Factor (HGF) for binding to Human Embryonic Kidney (HEK) and liver cell membrane fractions. Norleual also inhibits c-Met phosphorylation, Gab1 association and phosphorylation (Yamamoto and Elias et. al., submitted). Norleual shares high sequence homology with the hinge region of HGF and may be acting by binding to HGF and inhibiting HGF dimerization. Additionally, Norleual inhibits multiple HGF/c-Met functional effects in Madin-Darby Canine Kidney cells including scattering, migration, invasion, proliferation and urokinase-plasminogen activator induction (Elias et. al., submitted).

Figure 1a.



**Norleual Competes with HGF for binding and disrupts c-Met activation and downstream signaling in HEK 293 cells.** A. Mouse liver plasma membranes were incubated with 50 pM <sup>125</sup>I-HGF and indicated concentrations of HGF (■) or Norleual (△). B. HEK 293 cells were treated for 10 minutes with the indicated concentrations of HGF and Norleual. Lysates were immunoprecipitated for c-Met and the immunoprecipitates were probed for phospho-met and phospho-Gab1.

### ***The HGF/c-Met Receptor System***

HGF was originally identified in fibroblast-conditioned medium and named a “scatter factor” because of its ability to induce the disassociation and migration of epithelial cells. It was postulated that HGF must be a paracrine mediator of stromal/epithelial cell interactions in vivo (Balkovetz DF, 1998, *Mic Res Tech*). Subsequent to the discovery of HGF, numerous studies have shown that HGF is a pleiotropic growth factor that mediates an array of physiological and pathological mechanisms. For instance, cardiac remodeling is critically dependent on HGF (Nakamura T, 2005, *Am J Physiol Heart Circ Physiol*). Recently, it has been demonstrated that HGF is overexpressed in the tumor microenvironment causing an increase in tumor growth and metastases (Ide T, A, 2007, *Annals Surg Oncology*). Certain tumors, such as glioblastomas, demonstrate an autocrine HGF/c-Met loop and HGF blocking antibodies are effective at inhibiting the growth of these tumors in mice (Kim JK, 2006, *Clin Cancer Res*).

The receptor for HGF is the tyrosine kinase receptor, c-Met. C-Met is composed of a solvent-accessible alpha chain and a larger membrane-embedded beta chain. Upon binding HGF, c-Met undergoes autophosphorylation and dimerization, which initiates an intracellular signaling cascade that causes dramatic alterations in cell behavior. C-Met was originally identified from a chemically mutagenized osteosarcoma. This mutated form of c-Met was identified in the gastric tissue of gastric carcinoma patients and contributes to gastric carcinogenesis (Yu et. al., 1999, *Cancer*). Structurally, this

mutation confers constitutive expression and phosphorylation of c-Met due to the replacement of the extracellular and transmembrane domains with the translocated promoter (TPR) sequence. The information that the TPR sequence replaces in wildtype Met has been shown to contain the binding site for Cbl ubiquitin ligases, which targets proteins for metabolism (Mak H et. al., 2007, Oncogene). This finding sparked an effort to develop interventions for cancers characterized by aberrant c-Met expression. The SU11274 c-Met kinase inhibitor is one such agent, which induces apoptosis in TPR-Met transformed cells (Sattler M, 2003, Cancer Res). C-Met receptor antibodies and small molecule antagonists have shown promise in reducing tumor burden by acting at the level of the tumor cell and the endothelial cell to inhibit tumor growth and angiogenesis (Martens T, 2006, Clin Cancer Res). Met inhibitors are especially effective at reducing the growth of tumor cells that harbor aberrant forms of the c-Met receptor (Puri N, 2007, Clin Cancer Res).

In addition to its role in cancer, c-met plays a critical role in a variety of other processes including neurodevelopment, cardiovascular, hepatic, renal function, and wound healing. C-Met activation enhances long-term potentiation, synaptic plasticity, and has anti-fibrosis activity by reversing the effects of Transforming Growth Factor (Yang J, 2003, Am J Physiol and (Akimoto M et. al., 2004, Neuroscience). Studies demonstrating c-Met's role in wound healing have shown that HGF gene transfer accelerates dermal wound healing by stimulating angiogenesis and reepithelialization (Nakanishi K, 2002, Am J Path).

### ***MDCK Cells: The Classic Cellular Model for c-Met Activity***

MDCK cells were derived from the canine kidney in 1958 and have been an invaluable model for studying epithelial cell movement and polarity. Originally established and used in virology studies by Gaush (Gaush et. al., 1966, Proc Soc Exp Biol Med) these cells form compact colonies when grown at sub-confluent densities with tight intercellular junctions that prevent the passage of solutes between cells.

Treating MDCK cells with HGF disrupts colony formation by inducing chemokinetic migration. This phenomenon has been termed “scattering”, and it occurs in two stages. First, the cells lose their cell-cell contacts. Second, the cells migrate away from each other. In addition to its effect on random cell movement, an increasing concentration gradient of HGF can also stimulate the directional movement of a cell population, termed chemotaxis. Due to the effects of HGF on MDCK cell motility, it was speculated that HGF might have roles in development, wound healing, and cancer (Balkovetz DF, 1998, Mic Res Tech).

MDCK cells also undergo morphogenic changes when treated with HGF and this has provided a model for studying organ development in vitro. MDCK cell tubulogenesis is a morphogenic process induced by HGF where MDCK cells grown in collagen gels form branching tubular structures that sprout from cellular cysts. This model is reminiscent of HGF’s role in the development of organs such as the kidney, in which tubulogenesis occurs in the metanephric mesenchyme and the uteric bud (Stuart RO, 1995, Semin Nephrol).

These motogenic and morphogenic properties of MDCK cells are considered to be the gold standard for studying the HGF/c-Met pathway and for discovering c-Met inhibitors. Invasion, scattering, and tubulogenesis have been used to screen the geldanamycins for HGF/c-Met inhibition (Webb CP, 2000, Cancer Res). MDCK cell proliferation, scattering, and tubulogenesis were the chosen models for studying the antagonistic activity of the HGF/NK4 fragment (Kazuhiko D, 1997, FEBS Letters).

## **Part II**

### ***Wound Healing***

Wound healing is characterized as the process of restoring tissue that has been lost to traumatic injury. Inflammation, proliferation, and remodeling constitute the three dynamic and overlapping phases of wound healing.

When the skin is wounded, damaged capillaries in the denuded area leak blood into the wound, which leads to the formation of a fibrin clot. The fibrin clot serves to stop blood loss and provides a provisional matrix through which cells can migrate into the wounded area. In the initial inflammatory phase of wound healing, inflammatory cells migrate into the wound and phagocytose debris and bacteria to quell an infection. These cells release growth factors, such as TGF- $\beta$  and Platelet-Derived Growth Factor, that amplify the early wound healing process by activating resident fibroblasts, endothelial cells, and keratinocytes.

The inflammatory phase is followed by the proliferation phase in which the activated cells migrate and proliferate to initiate wound closure. Resident dermal



fibroblasts invade the wound and make a phenotypic transition to myofibroblasts that contract the wound. Additionally, the myofibroblasts deposit a collagen extracellular matrix. The tension exerted by the myofibroblasts on the collagen matrix causes a dramatic decrease in wound area and increase in wound strength. Concurrently, endothelial cells in the granulation tissue initiate wound angiogenesis causing an increase in blood flow. The increased blood supply to the wound provides oxygen and nutrients to the healing tissue. The keratinocytes that comprise the epithelium proliferate causing an increase in the thickness of the epithelium. The leading edge keratinocytes migrate, which reepithelializes the wound.

The remodeling phase lasts for several months and is characterized by further wound contraction, ECM deposition, and the formation of a scar. The remodeling phase is particularly important for increasing the strength of the wound although wounded skin never achieves the same strength of non-wounded skin. The resulting scar tissue is weaker than non-wounded skin due to inefficient cross-linking of the collagen fibrils. This difference between wounded and normal tissue highlights an important distinction between wound healing and tissue regeneration. This difference is illustrated well in fetal wounds, which heal perfectly, that is, the tissue regenerates to its previous strength and without a scar making the wound indistinguishable from non-wounded tissue. The ultimate goal of wound healing research is to understand how tissue regeneration happens and develop agents that promote its process in adults (Martin P, 1997, Science).

### ***Impaired Wound Healing***

Debilitating, chronic wounds are estimated to account for nearly 3 billion dollars in annual health care expenditures. It is impossible to estimate the additional cost due to the psychological and social damage caused by non-healing wounds. The consequence of a chronic wound is often the dysfunction or loss of the affected extremity. In fact, non-healing diabetic ulcers are the number one cause of non-traumatic amputations (National Diabetes Fact Sheet, 2003, CDC). As of yet, no single unifying factor has been identified that contributes to chronic non-healing wounds. Rather, chronic wounds are a result of impairments in a combination of the different phases of wound healing. For example, a pathological inflammatory response characterized by excessive neutrophil infiltration during the inflammatory phase and defective cellular function during the replication phase contributes to the formation of chronic wounds (De Mattei, *Dermatol Surg*, 2007 and Diegelmann, 2003, *Wound Rep Reg*).

One important distinction between normal and impaired wounds is the expression profile of proteases responsible for extracellular matrix (ECM) remodeling. The ECM serves as a support for cells in the wound environment and contains growth factors and proteases that modulate wound healing. The predominant ECM molecules in normal skin include the collagens, elastin, and proteoglycans. In wounded skin, fibrin and fibronectin are the major ECM proteins (Agren MS and Werthen M, 2007, *Int J Lower Ext Wounds*). The coordinated expression of proteases that regulate the expression of the ECM

proteins are fundamentally important to a normal wound healing response and this is illustrated in chronic wounds where the balance between ECM degradation and deposition is pushed in favor of degradation, which inhibits closure. The orchestrated expression of the matrix metalloproteinases (MMPs), which are a family of ECM-degrading proteases, is required for an effective wound healing response.

### ***MMPs***

MMPs are a family of endopeptidases that harbor a zinc or calcium ion in their active site. The MMP family consists of twenty-five different members, which are classified based on their substrate specificity into four groups: the collagenases, stromelysins, gelatinases, and non-soluble membrane-type MMPs (MT-MMPs). Their major function is tissue remodeling via ECM degradation. However, MMPs also regulate protein activity, and release growth factors from cell membranes and the ECM. MMP activity is critical to normal tissue architecture as has been demonstrated in a variety of normal and disease states. Under normal circumstances, MMP transcription, mRNA stability, and secretion are tightly regulated. However, if this regulation is lost, as is seen in many disease states, unregulated MMP activity can be deleterious.

An increase in net MMP activity during the first phase of wound healing is requisite for a normal healing response. However, MMP overexpression contributes to the impaired healing observed in chronic wounds. MMP-8 and

MMP-9 are upregulated in the anastomotic surgical line and contribute to wound failure (Agren, 2006, Surgery).

Additionally, a variety of global and specific MMP inhibitors prevent anastomotic leakage. The MMP inhibitor, doxycycline, increases the breaking strength and energy uptake of intestinal anastomoses (Pasternak, 2007, Int J Colorectal Dis). GM6001, a broad-spectrum MMP inhibitor, increases the breaking strength of incisional wounds, but inhibits secondary cutaneous wound healing (Mirastschijski, 2004, Exp Cell Res and Witte MB, 1998, Surgery). This effect is likely due to the temporal regulation of MMP activity during wound healing. The healing of excisional wounds, or healing by secondary intention, is characterized by an initial increase in net MMP activity, which is necessary for degrading the ECM surrounding the fibroblasts, endothelial cells, and keratinocytes that act in concert to close the wound. However, several studies including our own have observed an initial dehiscence of the excisional wound before wound closure commences (Elias et. al., submitted). This initial increase in wound area correlates with the increase in MMP activity in the wound itself. Therefore, it is possible that molecules, which increase wound strength and accelerate healing by primary intention, but inhibit healing by secondary intention act during this initial “lag” phase of wound healing. These treatment modalities hold particular promise for inhibiting incisional wound dehiscence and increasing wound strength in diabetic and obese patients that have undergone surgery.

## References

1. Wright JW and Harding JW. The brain angiotensin system and extracellular matrix molecules in neural plasticity, learning, and memory. *Progress in Neurobiology*. 2004; 72:263-293.
2. Handa R, Harding JW, and Simasko S. Characterization and Function of the Bovine Kidney Epithelial Angiotensin Receptor Subtype 4 using Angiotensin IV and Divalinal Angiotensin IV as Receptor Ligands. *The Journal of Pharmacology and Experimental Therapeutics*. 1999;291:1242-1249.
3. Zhang JH, Stobb JW, Hanesworth JM, Sardinia MF, and Harding JW. Characterization and Purification of the Bovine Adrenal Angiotensin IV Receptor (AT<sub>4</sub>) Using [<sup>125</sup>I]Benzoylphenylalanine-Angiotensin IV as a Specific Photolabel. *The Journal of Pharmacology and Experimental Therapeutics*. 1998;287:416-424.
4. Briand SI, Neugebauer W, and Guillemette G. Agonist-Dependent AT<sub>4</sub> Receptor Internalization in Bovine Aortic Endothelial Cells. *Journal of Cellular Biochemistry*. 1999;75:587-597.
5. Yamamoto BJ, Elias PD, Anderson ZJ, Masino AJ, Hudson BD, Varnum MD, Hosick HL, Wright JW, and Harding JW. Norleual, an AT<sub>4</sub> receptor ligand and c-met antagonist, represents a new class of anti-cancer drugs. Submitted to *Oncogene* in 2008.
6. Elias PD, Yamamoto BJ, Wright JW, and Harding JW. The angiotensin IV ligand, Norleual, inhibits hepatocyte growth factor (HGF)/c-met stimulated cellular

phenomena via the c-met-urokinase plasminogen activator (uPA) signaling pathway. Submitted to the Journal of Cell Science in 2008.

7. Balkovetz DF. Hepatocyte Growth Factor and Madin-Darby Canine Kidney Cells: in vitro models of epithelial cell movement and morphogenesis. *Microscopy Research and Technique*. 1998;43:456-463.

12. Nakamura T, Matsumoto K, Mizuno S, Sawa Y, Matsuda H, and Nakamura T. Hepatocyte growth factor prevents tissue fibrosis, remodeling, and dysfunction in cardiomyopathic hamster hearts. *American Journal of Heart and Circulatory Physiology*. 2005;288:2131-2139.

13. Ide T, Kitajima Y, Miyoshi A, Ohtsuka T, Mitsuno M, Ohtaka K, Miyazaki K. The hypoxic environment in tumor-stromal cells accelerates pancreatic cancer progression via the activation of paracrine hepatocyte growth factor/c-met signaling. *Annals of Surgical Oncology*. 2007;14:2600-2607.

14. Kim KJ, Wang L, Su Y, Gillespie GY, Salhotra A, Lal B, Laterra J. Systemic anti-hepatocyte growth factor monoclonal antibody therapy induces the regression of intracranial glioma xenografts. *Clinical Cancer Research*. 2006;12:1292-1298.

15. Yu J, Miehke S, Ebert M, Hoffman J, Breidert M, Alpen B, Starzynska T, Stolte M, Malfertheiner P, and Bayerdorffer E. Frequency of tpr-met rearrangement in patients with gastric carcinoma and in first-degree relatives. *Cancer*. 1999;88:1801-1806.

16. . Mak HHL, Peschard P, Lin T, Naujokas MA, Zuo D, and Park M. Oncogenic activation of the Met receptor tyrosine kinase fusion protein, Tpr-met,

involves exclusion from the endocytic degradative pathway. *Oncogene*. 2007;26:7213-7221.

17. Sattler M, Pride YB, Ma P, Gramlich JL, Chu SC, Quinnan LA, Shirazian S, Liang C, Podar K, Christensen JG, and Salgia R. A novel small molecule met inhibitor induces apoptosis in cells transformed by the oncogenic TRP-MET tyrosine kinase. *Cancer Research*. 2003;63:5462-5469.

15. Martens T, Schmidt N, Eckerich C, Fillbrandt R, Merchant M, Schwall R, Westphal M, and Lamszus K. A novel one-armed anti-c-met antibody inhibits glioblastoma growth *in vivo*. *Clinical Cancer Research*. 2006;12:6144-6152.

16. Puri N, Ahmed S, Janamanchi V, Tretiakova M, Zumba O, Krausz T, Jagadeeswaran R, and Salgia R. c-Met is a potentially new therapeutic target for treatment of human melanoma. *Clinical Cancer Research*. 2007;13:2246-2253.

17. Yang J, Liu Y. Delayed administration of hepatocyte growth factor reduces renal fibrosis in obstructive nephropathy. *AJP-Renal Physiology*. 2003;284:349-357.

18. Akimoto M, Baba A, Ikeda-Matsuo Y, Yamada MK, Itamura R, Nishiyama N, Ikegaya Y, and Matsuki N. Hepatocyte growth factor as an enhancer of NMDA currents and synaptic plasticity in the hippocampus. *Neuroscience*. 2004;128:155-162.

19. Nakanishi K, Uenoyama M, Tomita N, Morishita R, Kaneda Y, Ogihara T, Matsumoto K, Nakamura T, Maruta A, Matsuyama S, Kawai T, Aurues T, Hayashi T, and Ikeda T. Gene transfer of human hepatocyte growth factor into

rat skin wounds mediated by liposomes coated with sendai virus. *American Journal of Pathology*. 2002;161:1761-1772.

20. Gauth CR, Hard WL, and Smith TF. Characterization of an established line of canine kidney cells (MDCK). *Proceedings of the Society for Experimental Biology and Medicine*. 1966;122:931-935.

21. Stuart RO, and Nigam SK. Development of the tubular nephron. *Seminars in Nephrology*. 1995;15:315-326.

22. Webb CP, Hose CD, Koochekpour S, Jeffers M, Oskarsson M, Sausville E, Monks A, and Vande Woude GF. The geldanamycins are potent inhibitors of the hepatocyte growth factor/scatter factor-met-urokinase plasminogen activator-plasmin proteolytic network. *Cancer Research*. 2000;60:342-349.

23. Date K, Matsumoto K, Shimura H, Tanaka M, and Nakamura T. HGF/NK4 is a specific antagonist for pleiotrophic actions of hepatocyte growth factor. *FEBS Letters*. 1997;420:1-6.

25. Martin P. Wound healing-aiming for perfect skin regeneration. *Science*. 1997;276:75-80.

26. CDC, National Diabetes Fact Sheet: National Estimates and General Information on Diabetes in the United States. 1998, US Dept of Health and Human Services, Centers for Disease Control and Prevention. Atlanta, GA.

27. De Mattei M, Ongaro A, Magaldi S, Gemmati D, Legnaro A, Palazzo A, Masieri F, Pellati A, Catozzi L, Caruso A, and Zamboni P. Time and dose-dependent effects of chronic wound fluid on human adult dermal fibroblasts. *Dermatological Surgery*. 2007 [epub ahead of print].



27. Diegelmann RF. Excessive neutrophils characterize chronic pressure ulcers. *Wound Repair and Regeneration*. 2003;11:490-495.
29. Agren MS, and Werthen M. The extracellular matrix in wound healing: a closer look at therapeutics for chronic wounds. *The International Journal of Lower Extremity Wounds*. 2007;6:82-97.
30. Agren MS, Andersen TL, Mirastschijski U, Syk I, Schiodt CB, Surve V, Lindebjerg J, and Delaisse JM. Action of matrix metalloproteinases at restricted sites in colon anastomosis repair: an immunohistochemical and biochemical study. *Surgery*. 2006;140:72-82.
31. Pasternak B, Rehn M, Andersen L, Agren MS, Heegaard AM, Tengvall P, and Aspenberg P. Doxycycline-coated sutures improve mechanical strength of intestinal anastomoses. *International Journal of Colorectal Disease*. 2007;23:271-276.
32. Mirastschijski U, Haaksma CJ, Tomasek JJ, and Agren MS. Matrix metalloproteinase inhibitor GM 6001 attenuates keratinocyte migration, contraction and myofibroblast formation in skin wounds. *Experimental Cell Research*. 2004;299:465-475.
33. Witte MB, Thornton FJ, Kiyama T, Efron DT, Schulz GS, Moldawer LL, and Barbul A. Metalloproteinase inhibitors and wound healing: a novel enhancer of wound strength. *Surgery*. 1998;124:464-70.

## Chapter II

### **Manuscript I: To be submitted as a short report to the Journal of Cell Science.**

The Angiotensin IV (AngIV) Ligand, Norleual, inhibits Hepatocyte Growth Factor (HGF)/c-Met stimulated cellular phenomena via the c-Met-urokinase plasminogen activator (uPA) signaling pathway

Patrick Elias<sup>1,2\*</sup>, Brent Yamamoto<sup>2</sup>, Peter Meighan<sup>2,3</sup>, John Wright<sup>2,3</sup>, and Joseph Harding<sup>1,2,3</sup>.

\*Author for correspondence (email: pat@wsucougars.com)

<sup>1</sup>The Graduate Program in Pharmacology and Toxicology, Washington State University, Pullman, WA 99163, USA. <sup>2</sup>Pacific Northwest Biotechnology, LLC, Pullman, WA 99163, USA <sup>3</sup>Department of Veterinary Comparative Anatomy, Pharmacology & Physiology, Pullman, WA 99163, USA

**Summary:** Activation of the c-Met receptor by its cognate ligand, HGF, stimulates cell proliferation, motility, and morphogenesis. Each of these functions is critical for driving numerous physiologies ranging from organ development to tumor growth. Our laboratory has revealed that Norleual is a c-Met antagonist with potent anti-angiogenic and anti-tumorigenic activity (S.P. Yamamoto, unpublished). This study is the first to demonstrate that Norleual

blocks multiple c-Met stimulated cellular phenomena in Madin-Darby Canine Kidney (MDCK) cells. We provide direct evidence that these effects are via the inhibition of the c-Met-uPA signaling cascade.

## **Introduction**

This manuscript has been prepared in the format required by the journal of Cell Science. More information on formatting and submitting articles to the journal of cell science can be found at

<http://jcs.biologists.org/misc/submissions.shtml>.

Our laboratory and others have determined that AT<sub>4</sub> receptor ligands regulate numerous physiological processes including learning and memory consolidation, cardiovascular function, renal tubular physiology, and the local control of blood flow. The AT<sub>4</sub> receptor ligand, Nle<sup>1</sup>-AngIV, was identified as a physiological agonist based on its ability to facilitate learning and memory and Norleual was identified as an AT<sub>4</sub> receptor antagonist based on its ability to inhibit learning and memory (Wright et al., 1995). Further research from our laboratory demonstrated that <sup>125</sup>I-AngIV ligand binds irreversibly and with high affinity to multiple tissues and organs in vivo. High binding was particularly evident in aortic endothelial cells and cardiac fibroblasts. Subsequent to this discovery, our laboratory has completed numerous studies demonstrating that Norleual inhibits endothelial cell survival, angiogenesis, and tumor growth (S.P. Yamamoto, unpublished).

Studies of signal transduction pathways have shed light on the mechanisms of oncogenesis and tumor progression. What has been proven to be of critical importance is the role that the various receptor tyrosine kinases (RTKs) play in cancer progression. Structurally, the RTKs have an extracellular ligand binding domain, a membrane spanning domain, and a cytosolic C-terminal domain with tyrosine kinase activity. Binding of the extracellular domain by the ligand generates autophosphorylation of the kinase domain resulting in a series of signaling events that stimulates survival and motility. Examples of such RTKs that drive tumor progression include c-Kit, Eph, platelet derived growth factor receptor, vascular endothelial growth factor receptor, and c-Met (Ma et al., 2003). The role of c-Met in tumorigenesis has captured much attention after it was demonstrated that c-Met is overexpressed and mutated in very aggressive tumors and that this aberrant expression is correlated with metastatic progression and a poor prognosis. Currently, a one-armed antibody targeted at the c-Met receptor is in pre-clinical studies (Martens et al., 2006).

The ligand for c-Met is HGF, originally named for its potent growth and motility promoting activity in hepatocytes. HGF overexpression has been discovered in aggressive tumors and HGF neutralizing antibodies have been reported to be effective in inhibiting tumor growth in cell types with autocrine c-Met activation. Recently, the effectiveness of an HGF neutralizing antibody to inhibit U87 xenograft tumor growth has been demonstrated (Burgess et al., 2006).

Our laboratory has discovered that Norleual competes with HGF for binding to HEK293 cell and liver membrane fractions. Additionally, Norleual attenuates Gab1 association and phosphorylation in HEK293 cells (S.P. Yamamoto, unpublished). In this study, we demonstrate that Norleual attenuates multiple cellular responses in MDCK cells by blocking c-Met signalling. The results of this study provide additional insight into Norleual's anti-cancer mechanism of action.

## **Materials and Methods**

*Cell Proliferation:* 5000 MDCK cells were seeded into the wells of a 96 well plate in 10% FBS DMEM. To induce cellular quiescence, the cells were serum deprived for twenty-four hours prior to initiating the treatments. Following serum starvation, 10 ng/ml HGF alone and with various concentrations of Norleual or the PBS vehicle for controls was added to the media. The cells were allowed to grow under these conditions for four days and Norleual was added to the media everyday. On the fourth day, 1 mg/ml of 1-(4,5-Dimethylthiazol-2-yl)-3,5-diphenylformazan reagent (MTT, Sigma-Aldrich, MO) prepared in PBS was added to the cells and incubated for four hours. Dimethyl sulfoxide diluted in a 0.1 M glycine buffer was added to solubilize the cell membranes and the absorbance of reduced MTT in the buffer was quantitated at 590 nm on a plate reader. Control values were subtracted from all values to determine the increase in proliferation due to HGF treatment.

*Cell Scattering:* MDCK cells were grown to confluence on coverslips and pre-incubated for thirty minutes with  $10^{-10}$  molar Norleual at various concentrations before being stimulated with 20 ng/ml HGF. Cells were allowed to scatter off of the coverslips for 24-48 hours before being fixed with methanol and stained with Diff-Quik (Dade Behring, DE). The coverslips were removed from the plate and digital images of the cells that had scattered off of the coverslip were quantitated by densitometry using NIH Image J.

*Collagen I:* Rat tail type I collagen was prepared according to the protocol by Zamora et. al. (Zamora et al., 1980). Rat tail tendons were dissected out from adult rats immediately after sacrifice and sterilized in 70% ethanol for 30 minutes. After sterilization, 1 g of tendons was solubilized in 100 ml of 0.5 M acetic acid with stirring for 48 hours at 4°C. The dissolved tendons were centrifuged at 2000 g for twenty minutes to remove any insoluble material. The clarified supernatant was then dialyzed against 4 L of water for 4 days at 4°C. The collagen I gelling solution consisted of a 1:1:1 mixture of 10X MEM, 0.1 N NaOH, and 1 M NaHCO<sub>3</sub>. To induce gelation, a 1:5 dilution of gelling solution to collagen was made and incubated at 37°C for 30 minutes.

*Cell Invasion/Migration:* The inside of the BD Falcon cell culture inserts for 24 well plates (BD Biosciences, CA) were coated with 50 µl of 2 mg/ml of neutralized collagen I. For the invasion assay, the collagen I was allowed to gel at 37 degrees Celsius. In the migration assay, no extracellular matrix barrier was applied to the insert, but rather the cells were evaluated for their ability to migrate in the presence of HGF and Norleual. 50,000 MDCK cells were added to the

inside of the inserts and allowed to attach to the collagen for two hours before adding 20 ng/ml of HGF alone or in combination with Norleual to the bottom chamber to stimulate migration. Norleual or the PBS vehicle was added to the inside chamber as well. The cells were allowed to invade the collagen and migrate to the underside of the chamber under these treatment conditions for eight hours. The cells that had invaded the collagen and migrated to the underside of the membrane were fixed with 100% methanol for 10 minutes at room temperature. The non-migrated cells remaining on the inside of the insert were wiped away with a cotton swab and the migrated cells on the bottom of the insert were stained with Diff-Quik (Dade Behring, DE). The cells that invaded the collagen and migrated to the underside of the membrane were counted in five random fields at 20x objective on a light microscope.

*Phospho-Erk western blots:* MDCK cells were seeded in 100 mm tissue culture plates and grown to 95% confluency in DMEM containing 10% FBS. The cells were serum deprived for 24 hours prior to the treatment to reduce phospho-erk to basal levels. Following serum starvation, cocktails comprised of vehicle, 10 ng/ml HGF alone, 10 ng/ml HGF and  $10^{-10}$  M Norleual, and 10 ng/ml HGF and  $10^{-12}$  M Norleual were prepared and pre-incubated for 90 minutes at room temperature. The cocktail was added to the cells for 10 minutes to stimulate the c-Met receptor and downstream proteins. The cells were lysed in ice-cold Ripa buffer with protease and phosphatase inhibitors. The lysate was clarified by centrifugation at 15,000 g for 15 minutes, diluted with 2x reducing Laemmli buffer and boiled for ten minutes at 95° C. 20 µl of lysate was

electrophoresed on a poly-acrylamide gel, transferred to nitrocellulose, and blocked in Tris-buffered saline (TBS) with 5% milk for one hour at room temperature. The phospho-ERK antibody (Santa Cruz Biotechnology, CA) and total ERK antibody (Santa Cruz Biotechnology, CA) was added to the blocking buffer at a final concentration of 1:1000 and incubated at 4° C overnight with gentle agitation. The membranes were washed several times with TBS and a 1:5000 concentration of horseradish-peroxidase conjugated goat anti-rabbit was added to the blocking buffer and the membranes were incubated for one hour at room temperature. The membranes were washed several times with TBS before being developed by chemiluminescence and the bands were detected on a chemiluminescence imager.

*uPA Activity Assay:* 5000 MDCK cells were seeded in 96 well plates in 100 µl of 1% FBS DMEM to induce quiescence. The MDCK cells were stimulated with 10 ng/ml HGF in the presence or absence of various concentrations of Norleual. After 24-48 hours of treatment, uPA activity was quantitated with the uPA activity assay kit (Millipore, MA) according to the manufacturers instructions. After 24-48 hours of treatment, 10 µl of assay buffer and 10 µl of the chromogenic tripeptide substrate was added to the media and incubated for four hours at 37°C. Absorbance was quantitated at 405 nm on a Biotek plate reader. Control values were subtracted from all values to determine HGF-induced uPA activity.

*Statistical Analysis:* Groups of three treatments or more were analyzed with one-way ANOVA with Tukey's post-hoc analysis to determine differences



between a specific treatment and control. Data is presented as the mean +/- s.e.m. with  $p \leq 0.05$  considered statistically significant. All data was analyzed with Prism statistical software.

## **Results & Discussion**

### *Norleual Attenuates HGF/c-Met stimulated MDCK cell proliferation.*

MDCK cells are the chosen model for studying c-Met mediated biological effects because they undergo dramatic changes in proliferation, motility, and morphology when treated with HGF (Stella and Comoglio, 1999). The stimulation of cell proliferation by HGF/SF provides a model for c-Met's role in tumor growth. The increased proliferation during HGF/SF treatment is due to the stimulation of the Ras/Raf/Mek pathway downstream of c-Met activation. The Ras/Raf/Mek pathway transduces signals from the plasma membrane to the nucleus, activating transcription factors that increase cell division. The adaptor protein, Shc, associates with the cytoplasmic tail of c-Met through its SH2 domain. Shc activates Grb2, which in turn activates SOS, triggering the activation of the Ras/MAPK pathway (Zhang and Vande Woude, 2003). In addition to controlling cell proliferation, this pathway has also been shown to be indispensable for cell invasion and morphogenesis (Ishibe et al., 2003).

It has been previously demonstrated by our lab that Norleual has dramatic effects on tumor cell proliferation in vitro and in vivo (S.P. Yamamoto, unpublished). However, until now the mechanism by which Norleual inhibited tumor cell proliferation had not been elucidated. Fig. 1 shows that Norleual

attenuates HGF/SF stimulated cell proliferation, which explains Norleuals potent anti-cancer activity in vivo.

*Norleual is a potent inhibitor of MDCK cell invasion and migration.*

Previous studies from our lab have demonstrated that Norleual is able to inhibit +SA murine mammary tumor and B16 melanoma metastases (S.P. Harding, unpublished). It has been well established that c-Met overexpression in tumors results in metastases (Ferraro et al., 2006). Stimulating MDCK cells with HGF causes the cells to transition from their flattened morphology to an invasive phenotype characterized by a decrease in cell-cell and cell-ECM adhesion, and an increase in pseudopodia (Vadnais et al., 2002). This increase in the invasive potential of the cells provides a model for c-Met's role in tumor metastases. In order for tumor cells to metastasize, they must detach from their substrate, stay viable in suspension, and reattach to a distant organ. The cell is then stimulated by chemotactic cues from the surrounding stroma to invade the organ. HGF is one such chemotactic agent secreted from the mesenchyme, which upon activating c-Met, promotes invasion. The intracellular signaling to stimulate invasion is carried out by activated Met, which phosphorylates Gab1 at several tyrosine residues that are essential for recruiting downstream SH2 and SH3 domain containing effectors, such as PI3-Kinase (PI3-K). PI3-K phosphorylates Akt , which activates transcription factors. The activated transcription factors translocate to the nucleus and initiate the transcription of genes required for invasion. The PI3-K/Akt pathway is essential for HGF mediated cell motility because treatment with the PI3-K inhibitor, wortmannin, in HGF/SF treated cells

abrogates cell scattering (Royal and Park, 1995). As shown in Fig. 2a and 2b, picomolar concentrations of Norleual inhibit MDCK cell invasion and migration.

*Norleual inhibits HGF/SF/c-Met mediated cell scattering in MDCK cells.*

When MDCK cells are grown at a low cell density they form colonies and the cells demonstrate a “cobblestone” morphology, which is characterized by tight intercellular junctions. The scattering of MDCK cells occurs in two stages. First, the cells lose their cell-cell adhesion and become polarized. Second, they separate completely and migrate away from each other. This c-Met driven process has been shown to be dependent on the activation of the Ras/Raf/Mek and PI3-K/Akt pathway as pharmacological inhibitors of these pathways inhibit scattering (Royal and Park, 1995; Liang et al., 2001).

We reasoned that Norleual effect on proliferation and motility suggests that it should also inhibit cell scattering. We developed a quantitative assay to analyze cell scattering where cells were plated on plastic coverslips in six well plates and allowed to grow to 100% confluency. In the absence of HGF, the MDCK cells grow as a compact monolayer on the coverslips. When the MDCK cells are treated with HGF, they scattered off of the coverslips on to the plate leaving a ring of cells on the plate. The area of cells that have scattered off of the coverslip and on to the plate can be quantitated with densitometry. When we treated MDCK cells with HGF and 0.1 nM Norleual, Norleual inhibited MDCK cell scattering off of the coverslip.

*Norleual disrupts c-Met signaling.* It has been demonstrated that c-Met driven migration and invasion require the activation of the c-Met-uPA signaling

axis. Particularly, uPA induction is indispensable for c-Met biological effects as application of the uPA inhibitor, B428, inhibits c-Met mediated proliferation (Webb et al., 2000). Activation of the MEK/ERK pathway downstream of c-Met activation is requisite for the biological responses of c-Met as MEK/ERK inhibitors block uPA induction and subsequent cellular functions (Lee et. al., 2006).

We reasoned that Norleual's ability to inhibit invasion, scattering, and proliferation is by blocking c-Met signalling. To test this hypothesis, we evaluated changes in phospho-ERK expression induced by HGF in the absence and presence of Norleual. MDCK cells were treated for ten minutes with HGF and phospho-ERK was detected by western blotting. As shown in Fig. 4, ERK activation by HGF was suppressed by Norleual treatment.

To analyze uPA activity, we first generated a dose-response curve with HGF to determine the sub-maximal concentration of HGF required to stimulate uPA activity above controls. As shown in fig. 5a, 10 ng/ml of HGF was the lowest concentration tested that stimulated uPA activity. Fig. 5b demonstrates that when 10 ng/ml HGF and 0.1 nM Norleual were added together, there was significant attenuation of uPA activity. However, 0.1 nM Norleual was able to reduce uPA activity even at saturating concentrations of HGF (Fig. 5c).

HGF/c-Met signaling activates a number of cellular responses triggering the transition to a metastatic phenotype. The biological functions that are most relevant to c-Met's role in tumor progression are proliferation, migration, invasion, and scattering. Many studies have shown that HGF/c-Met activation has

mitogenic and invasive activity on ovarian, glioma, gastric, and lung carcinomas (Sawada et al., 2007; Eckerich et al., 2007; Lee et al., 2006; Ma et al., 2007).

The demonstrated ability of Norleual to inhibit c-Met signaling and consequent biological effects makes it a promising molecule in the treatment of aggressive cancers where c-Met is overexpressed or mutated.

Activation of the c-Met receptor has been shown to be required for tumor cell invasion and metastases in multiple cancers. For example, the role of c-Met in melanoma cell proliferation was shown in siRNA treated melanoma cells, in which there was a 60% reduction in melanoma cell proliferation (Neelu et. al., 2007). Additionally, elevated c-Met expression is correlated with a poor prognosis in many malignancies. Highly invasive cancers, such as metastatic breast cancer, express c-Met at levels well above poorly aggressive cancers (Parr et al., 2001). In addition to elevated expression, multiple isoforms of c-Met contribute to malignancy. These include mutations in the tyrosine kinase domain of c-Met, which confers constitutive phosphorylation of the receptor. Some examples of cancers that harbor the tyrosine kinase mutation are hepatocellular carcinoma, head and neck squamous cell carcinoma, glioma, and papillary renal carcinomas (Ma et al., 2003). However, mutations in c-Met are not exclusive to the tyrosine kinase domain. The juxtamembrane domain is critical for the metabolism of c-Met as mutations in this domain inhibit ubiquination, ultimately increasing receptor expression at the cell surface (Lee et al., 2006). The increase in c-Met expression drives oncogenesis by increasing the sensitivity to

HGF stimulation (Corso et al., 2005). We are currently exploring the potential for Norleual to have activity against cells that harbor aberrant forms of c-Met.

Similarly to c-Met, high uPA expression in the urine of cancer patients is correlated with a poor prognosis. UPA is a protease that activates the plasminogen proteolytic cascade to produce the zymogen plasmin. Plasmin activates matrix metalloproteinases (MMPs) to increase invasion, but can also modulate the ECM independent of MMPs to drive tumor cell invasion. UPA is absolutely critical for c-Met mediated invasion as application of short-hairpin RNA for uPA in the stomach cancer cell line, NUGC-3, decreases c-Met stimulated cell invasion (Lee et al., 2006). For this reason, Norleual may represent an important therapeutic candidate as an anti-invasive drug in a variety of invasive cancers where c-Met stimulated uPA activity is driving tumor progression.

It should not be overlooked that there are other receptor systems that modulate c-Met activity and subsequent downstream signaling. These receptors include the epidermal growth factor receptor, Fas, CD44, integrin  $\alpha6\beta4$ , Plexin B, ErbB2, and Ron (Corso et. al., 2005). Each of these receptors interacts with c-Met to amplify the signaling response, regulate cell survival and invasive growth. Future studies from our laboratory are focused at studying the involvement of these receptors in determining Norleual's mechanism of action.

### **Acknowledgements**

Pacific Northwest Biotechnology, LLC, provided the funding for this study.

## References:

1. **Burgess, T., Coxon, A., Meyer, S., Sun, J., Rex, K., Tsuruda, T., Chen, Q., Ho, S., Li, L., Kaufman, S., McDorman, K., Cattley, R.C., Sun, J., Elliott, G., Zhang, K., Feng, X., Jia, X., Green, L., Radinsky, R., and Kendall, R.** (2006) Fully Human Monoclonal Antibodies to Hepatocyte Growth Factor with Therapeutic Potential against Hepatocyte Growth Factor/c-Met-Dependent Human Tumors. *Cancer Res.* **3**, 1721-1729.
2. **Corso, S., Comoglio, P.M., and Giordano, S.** (2005) Cancer therapy: can the challenge be MET? *TRENDS Mol. Med.* **6**, 284-292.
3. **Eckerich, C., Zapf, S., Fillbrandt, R., Loges, S., Westphal, M., and Lamszus, K.** (2007) Hypoxia can induce c-Met expression in glioma cells and enhance SF/HGF-induced cell migration. *Int. J. Cancer* **121**, 276-283.
4. **Ferraro, D., Corso, S., Fasano, E., Panieri, E., Santangelo, R., Borrello, S., Giordano, S., Pani, G., and Galeotti, T.** (2006) Pro-metastatic signaling by c-Met through RAC-1 and reactive oxygen species (ROS). *Oncogene* **25**, 3689-3698.
5. **Ishibe, S., Joly, D., Zhu, X., Cantley, L.G.** (2003) Phosphorylation-Dependent Paxillin-ERK Association Mediates Hepatocyte Growth Factor-Stimulated Epithelial Morphogenesis. *Mol. Cell* **12**, 1275-1285.
6. **Lee, J.H., Gao, C.F., Lee, C.C., Kim, M.D., and Vande Woude, G.F.** (2006) An alternatively spliced form of Met receptor is tumorigenic. *Exp. Mol. Med.* **5**, 565-573.

7. **Lee, K.H., Choi, E.Y., Hyun, M.S., Jang, B.I., Kim, T.N., Kim, S.W., Song, S.K., Kim, J.H., Kim, J.R.** (2006) Hepatocyte growth factor/c-met signaling in regulating urokinase plasminogen activator in human stomach cancer: A potential therapeutic target for human stomach cancer. *Korean J. Intern. Med.* **1**, 20-27.
8. **Liang, C.C., and Chen, H.C.** (2001) Sustained Activation of Extracellular Signal-regulated Kinase Stimulated by Hepatocyte Growth Factor Leads to Integrin  $\alpha_2$  Expression That is Involved in Cell Scattering. *J. Biol. Chem.* **24**, 21146-21152.
9. **Ma, P.C., Maulik, G., Christensen, J., and Salgia, R.** (2003) c-Met: Structure, functions and potential for therapeutic inhibition. *Cancer Metastasis Rev.* **22**, 309-325.
10. **Ma, P.C., Tretiakova, M.S., Nallasura, V., Jagadeeswaran, R., Husain, A.N., and Salgia, R.** (2007) Downstream signaling and specific inhibition of c-Met/HGF pathway in small cell lung cancer: implications for tumour invasion. *Br. J. Cancer* **97**, 368-377.
11. **Martens, T., Schmidt, N., Eckerich, C., Fillbrandt, R., Merchant, M., Schwall, R., Westphal, M., and Lamszus, K.** (2006). A Novel One-Armed Anti-c-Met Antibody Inhibits Glioblastoma Growth In Vivo. *Clin. Cancer Res.* **20**, 6144-6152.
12. **Neelu, P., Ahmed, S., Janamanchi, V., Tretiakova, M., Zumba, O., Krausz, T., Jagadeeswaran, R., and Salgia, R.** (2007) c-Met Is a



- Potentially New Therapeutic Target for Treatment of Human Melanoma.  
*Clin. Cancer Res.* **7**, 2246-2253.
13. **Parr, C., and Jiang, W.G.** (2001) Expression of hepatocyte growth factor/scatter factor, its activator, inhibitors and the c-Met receptor in human cancer cells. *Int. J. Oncol.* **4**, 857-863.
14. **Qinghua, Z., Chen, S., You, Z., Yang, F., Carey, T.E., Saims, D., and Wang, C.** (2002). Hepatocyte Growth Factor Inhibits Anoikis in Head and Neck Squamous Cell Carcinoma Cells by Activation of ERK and Akt Signaling Independent of NFkB. *J. Biol. Chem.* **28**, 25203-25208.
15. **Royal, I., and Park, M.** (1995) Hepatocyte Growth Factor-induced Scatter of Madin-Darby Canine Kidney Cells Requires Phosphatidylinositol 3-Kinase. *J. Biol. Chem.* **46**, 27780-27787.
16. **Sawada, K., Radjabi, A.R., Shinomiya, N., Kistner, E., Kenny, H., Becker, A.R., Turkyilmaz, M.A., Salgia, R., Yamada, S.D., Vande Woude, G.F., Tretiakova, M.S., and Lengyel, E.** (2007). c-Met Overexpression is a Prognostic Factor in Ovarian Cancer and an Effective Target for Inhibition of Peritoneal Dissemination and Invasion. *Cancer Res.* **67**, 1670-1679.
17. **Stell, M.C., and Comoglio, P.M.** (1999). HGF: a multifunctional growth factor controlling cell scattering. *Int. J. Biochem. Cell Biol.* **31**, 1357-1362.
18. **Vadnais, J., Nault, G., Daher, Z., Amraei, M., Dodier, Y., Nabi, I.R., and Noel, J.** (2002). Autocrine Activation of the Hepatocyte Growth Factor

- Receptor/Met Tyrosine Kinase Induces Tumor Cell Motility by Regulating Pseudopodial Protrusion. *J. Biol. Chem.* **50**: 48342-48350.
19. **Wright, J.W., Krebs, L.T., Stobb, J.W., and Harding, J.W.** (1995). The Angiotensin IV System: Functional Implications. *Front. Neuroendocrinol.* **16**, 23-52.
20. **Zamora, P.O., Danielson K.G., and Hosick, H.L.** (1980) Invasion of Endothelial Cell Monolayers on Collagen Gels by Cells from Mammary Tumor Spheroids. *Cancer Res.* **40**, 4631-4639.
21. **Zhang, Y., and Vande Woude, G.F.** (2003). HGF/SF-Met Signaling in the Control of Branching Morphogenesis and Invasion. *J. Cell Biochem.* **88**, 408-417.

## Figure Legends

### **Figure 2. Norleual attenuates HGF/c-Met proliferation.**

MDCK cells were stimulated with PBS vehicle (controls), HGF, or HGF in combination with Norleual. The cells were allowed to grow under these treatment conditions for four days. Cell viability was determined on the fourth day by MTT assay. Control values were subtracted from all values to determine the HGF-induced increase in cell proliferation. N=6, mean +/- s.e.m. \* indicates  $p < 0.05$  vs control as determined by Tukey's post-hoc analysis.

### **Figure 3. Norleual inhibits MDCK cell invasion and migration.**

MDCK cells were seeded on top of collagen gels in the upper compartment (a) or in the upper compartment without a collagen barrier (b) of a transwell chamber and stimulated to migrate to the underside of the membrane with PBS (controls), 10 ng/ml HGF, or 10 ng/ml HGF in combination with Norleual. N=3, mean +/- s.e.m. \* indicates  $p < 0.05$  vs. control by Tukey's post-hoc analysis.

### **Figure 4. Norleual inhibits MDCK cell scattering.**

MDCK cells were grown to 100% confluence on coverslips. The cells were stimulated to scatter off of the coverslip by adding 20 ng/ml of HGF to the media. After 24 hours of scattering, the cells were fixed with methanol and stained with Diff-Quik (Dade Behring). The coverslips were removed to reveal the ring of cells that had scattered off of the coverslip and onto the plate. The effect of HGF on

scattering was quantitated by determining the densitometry of the scattered cells from digital images. N=4, mean +/- s.e.m.. \*indicates p<0.05 vs. control by Tukey's post-hoc analysis.

**Figure 5. Norleual blocks ERK activation by HGF/c-Met.**

MDCK cells were plated in 100 mm plates and grown to 95% confluency. Following serum deprivation, the cells were stimulated with 10 ng/ml HGF alone and with Norleual. N=3, mean +/- s.e.m. \* indicates p<0.05 vs. control by Tukey's post-hoc analysis.

**Figure 6. Norleual perturbs HGF/c-Met uPA induction.**

MDCK cells in 96 well plates were stimulated with either 10 ng/ml, 20 ng/ml, or 40 ng/ml HGF (a). Norleual attenuated 10 ng/ml HGF uPA induction (b) and 40 ng/ml HGF uPA induction (c). N=6, mean +/- s.e.m.

\* indicates p<0.05 vs. control by Tukey's post-hoc analysis.

Figure 2.

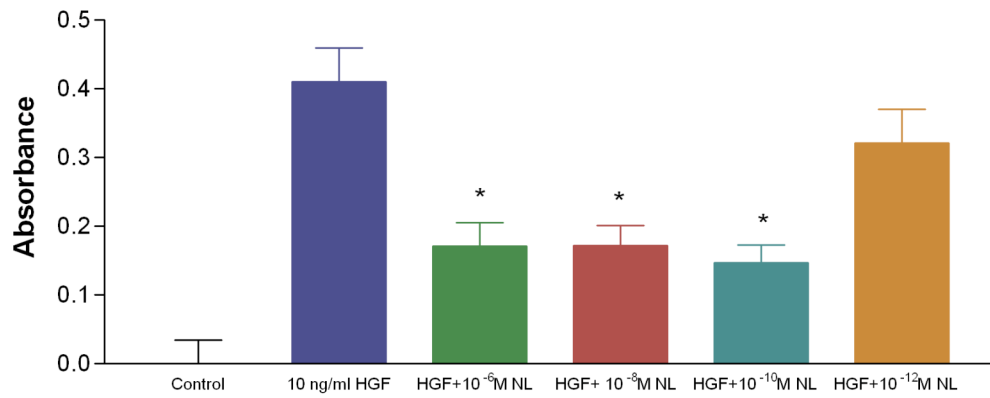
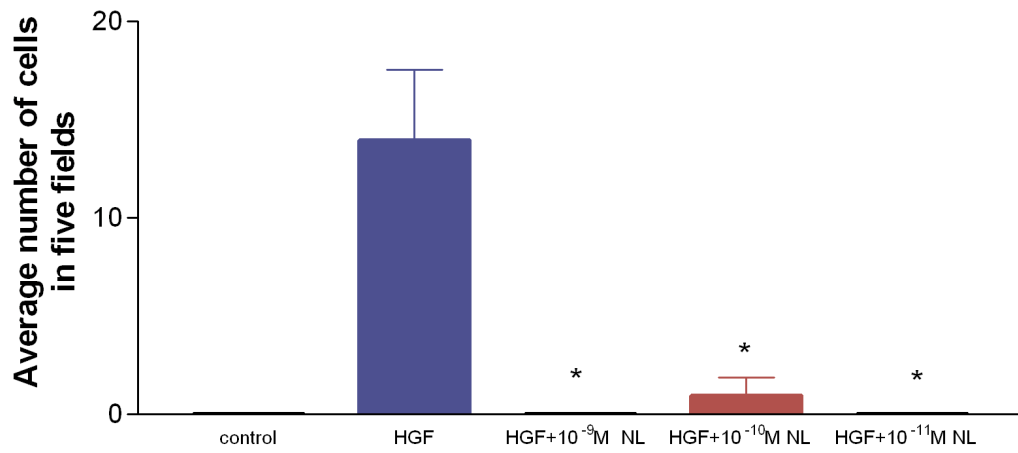


Figure 3

a.



b.

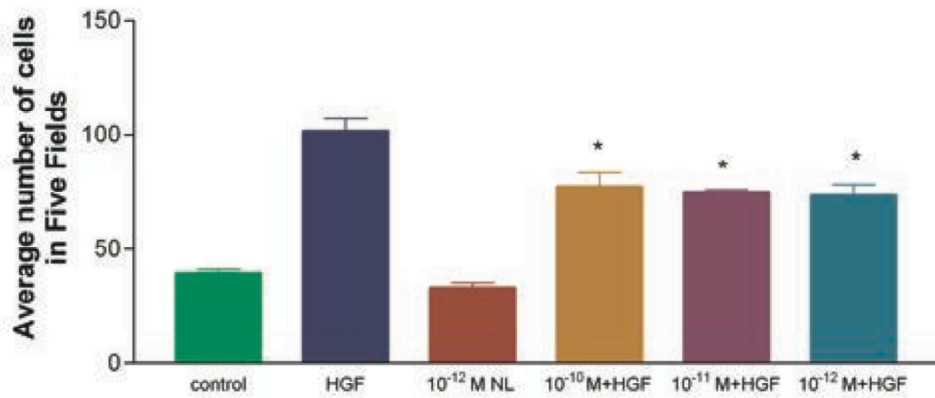


Figure 4.

Control

HGF

HGF+ $10^{-10}$  M NL

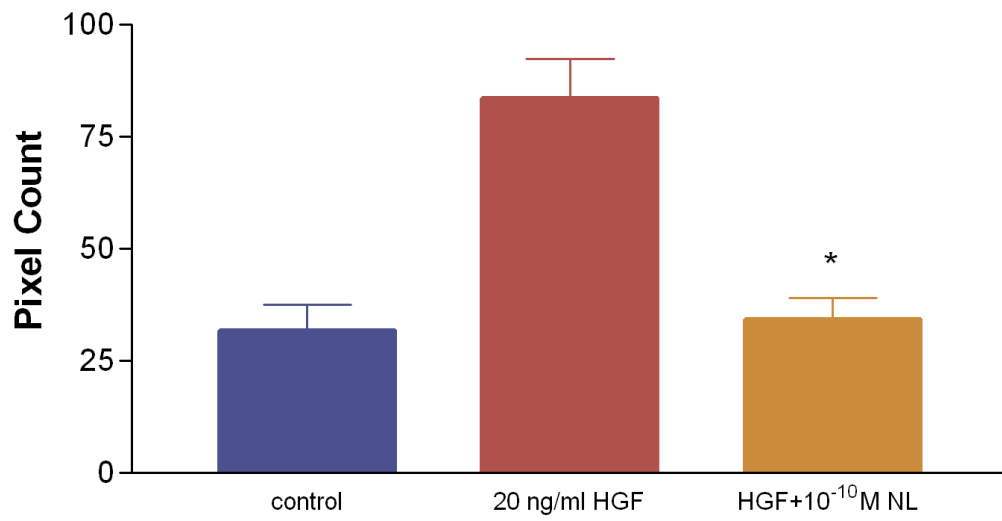
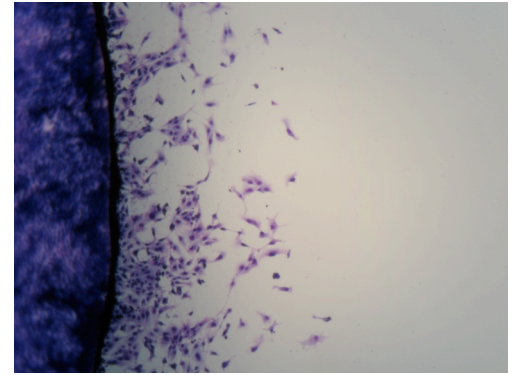
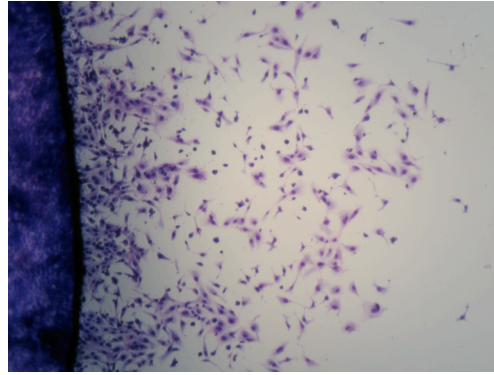
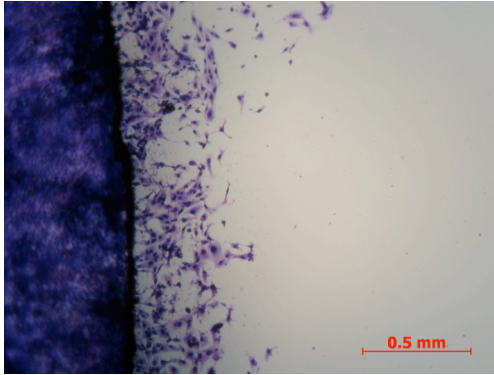


Figure 5.

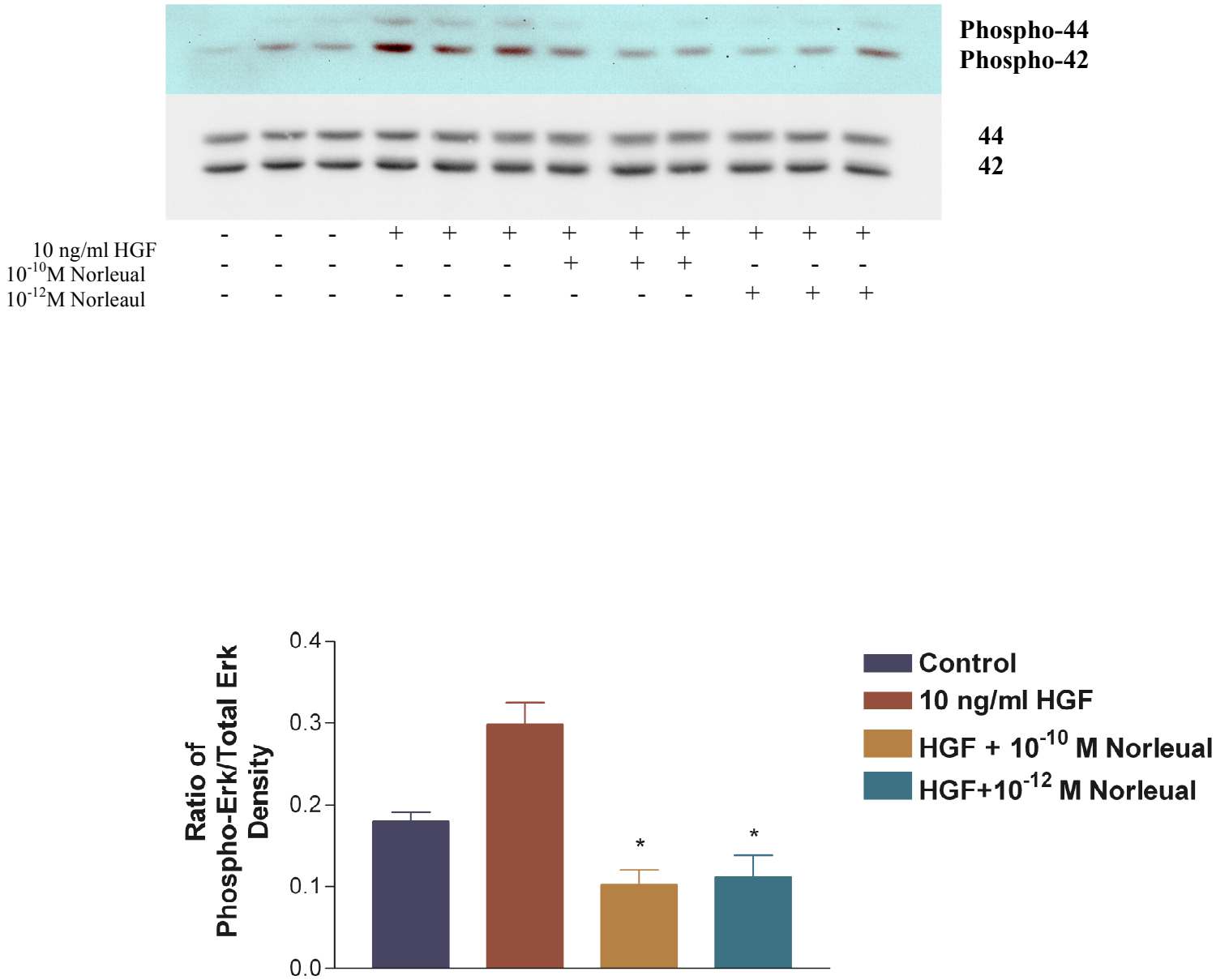
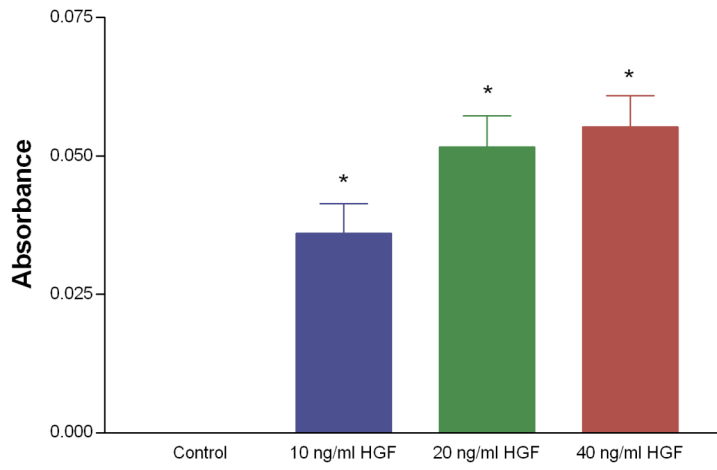
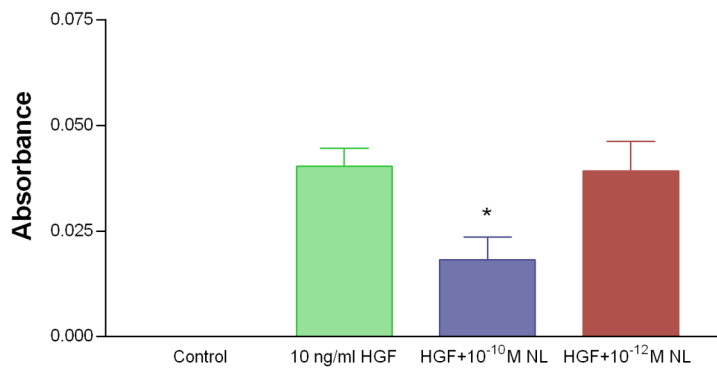


Figure 6.

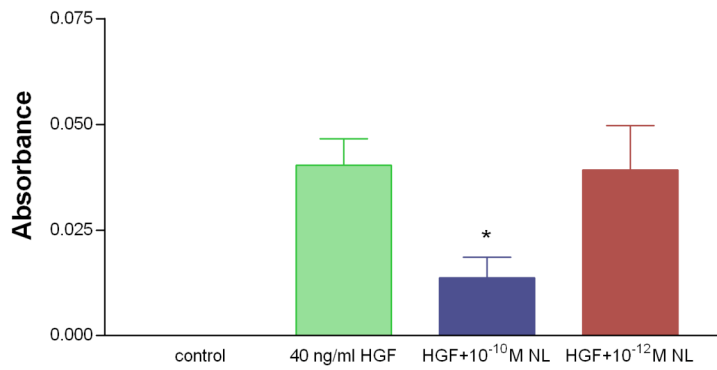
a.



b.



c.





## Chapter III

**Manuscript II:** Submitted as an original research article to the Journal of Wound Repair and Regeneration

The Angiotensin IV (AngIV) Ligand, Nle<sup>1</sup>-Angiotensin IV (Nle<sup>1</sup>-AngIV), Accelerates Dermal Wound Repair

Patrick D. Elias, PhD; Mohamed Jabbes, PhD; Bonnie G. Campbell, D.V.M., PhD; Joseph W. Harding, PhD; and John W. Wright, PhD

From Pacific Northwest Biotechnology, LLC, Pullman, WA.

Reprint requests: Patrick D. Elias, Pacific Northwest Biotechnology, 1425 NE Terre View Drive, Pullman, WA 99163. Fax:(509) 332-8095; Email: pat@wsucougars.com.

**Abstract:** Previous studies report that angiotensin II (AngII) and angiotensin (1-7) (Ang1-7) accelerate dermal wound repair. In this study, the AngIV receptor ligand, Nle<sup>1</sup>-AngIV, facilitates dermal wound healing in both normal and impaired models as evidenced by the inhibition of excisional wound dehiscence, the enhancement of incisional wound strength, and reduction in incisional wound dehiscence. In addition, Nle<sup>1</sup>-AngIV stimulates dermal fibroblast migration, proliferation, and wound healing, cell functions that heal the dermis *in vivo*. Nle<sup>1</sup>-AngIV may increase collagen deposition in the wound by decreasing MMP-2 activity.

### Introduction

This manuscript has been prepared in the format required by the journal of wound repair and regeneration. Additional information for formatting and

submitting articles to the journal of wound repair and regeneration can be found at <http://www.blackwellpublishing.com/submit.asp?ref=1067-1927&site=1>.

Classical angiotensins were characterized based on their ability to modulate blood pressure, body water balance, and cyclic regulation of reproductive hormones and behaviors. These effects are predominantly mediated by the AT<sub>1</sub> receptor, which binds AngII and AngIII. In 1993, our laboratory discovered a distinct binding site for AngII (3-8), a fragment of AngII referred to as AngIV. Subsequent to this finding, it was demonstrated that the receptor for AngIV is ubiquitously expressed and plays an important role in variety of classic physiological and behavioral states, including learning and memory, cardiovascular function, exploratory behavior, the local regulation of blood flow, and renal function.<sup>1</sup>

Evidence for AngII effect on wound healing came from the discovery that AngII receptors are enhanced in the dermis during experimental wound healing.<sup>2</sup> Several studies, which have explored the mechanism by which AngII stimulates tissue repair have discovered that AngII stimulates endothelial survival, migration, angiogenesis, as well as migration in smooth muscle cells, and fibroblasts.<sup>3,4,5</sup> Other studies have indicated that AngII activates growth factor receptors, such as epidermal growth factor and platelet-derived growth factor both of which are integral to the tissue repair process.<sup>6</sup> AngII is also capable of altering ECM architecture by increasing collagen I expression.<sup>7</sup>

Recent studies have revealed that a fragment of AngII, Ang(1-7), also accelerates dermal wound repair. Ang(1-7) has been demonstrated to increase

incisional and excisional wound closure in normal and diabetic mice, and increase the viability of random flaps in a rodent model.<sup>5</sup> The mechanisms for the effect of Ang(1-7) on wound repair include an increase in the proliferation and thickness of the epithelium, proliferation of epidermal stem cells, and increased ECM deposition.<sup>5,8</sup>

This study evaluates the ability of Nle<sup>1</sup>-AngIV, an AT<sub>4</sub> receptor ligand, to facilitate wound healing. The data presented in this study indicates that Nle<sup>1</sup>-AngIV inhibits excisional wound dehiscence during the first week of wound healing, increases the breaking strength of incisional wounds, accelerates scab release, and decreases the area of wound dehiscence in type 2 diabetic obese mice. In addition, the dermis in the incisional wounds of the Nle<sup>1</sup>-AngIV treated animals is healed earlier than controls.

## **Methods**

*Cell Culture and Reagents:* Human Foreskin fibroblasts (HFFs) were purchased from the American Type Culture Collection and cultivated in 10% Fetal Bovine Serum in Dulbecco's Modified Eagle's Medium. The Bioanalytical Laboratory at Washington State University synthesized Nle<sup>1</sup>-AngIV.

*WST-8 Proliferation Assay:* The WST-8 assay was performed according to the manufacturers instructions (Biovision Inc. Mountain View, CA). 5000 HFFs were seeded into each well of a 96 well plate in complete growth media. After the cells had attached to the dish, Nle<sup>1</sup>-AngIV prepared fresh in sterile PBS with 0.1% BSA was added to the media and the cells were allowed to proliferate

for 24 hours. Controls received sterile PBS with 0.1% BSA only. After 24 hours of treatment, 10  $\mu$ l of WST-8 was added to the wells and incubated for four hours at 37 degrees Celsius. The absorbance was quantitated on a Biotek plate reader at 440 nm.

*HFF Migration Assay:* 50,000 HFFs were seeded into the top chamber of a 24 well Falcon cell culture insert (BD Biosciences, San Jose, CA) chamber in 1% FBS DMEM and allowed to attach to the insert for two hours at 37 degrees Celsius. After the cells adhered to the insert, 700  $\mu$ l of 1% FBS DMEM with either the vehicle (sterile PBS with 0.1% BSA) or Nle<sup>1</sup>-AngIV was added to the bottom chamber. The same concentration of Nle<sup>1</sup>-AngIV was added to the media in the top chamber. The cells were allowed to migrate for four hours before they were fixed with 100% methanol for ten minutes at room temperature. After the cells were fixed, they were stained with Diff-Quik (Dade Behring, Newark, DE). The cells remaining on the inside of the insert were carefully removed with a cotton swab. The cells that had migrated to the underside of the membrane were counted in five random fields at 20x on a light microscope.

*HFF Wound Healing Assay:* HFFs were seeded onto Falcon Integrid petri dishes (BD Biosciences, San Jose, CA) in 10% FBS DMEM and allowed to grow to 100% confluency. The confluent monolayer was wounded using a pipet tip. The cells were washed two times with sterile PBS to wash away cell debris and constituents released by the wounding. The media was replaced with fresh 10% DMEM with addition of either the PBS vehicle or Nle<sup>1</sup>-AngIV. The HFFs were

allowed to invade the wounded area and a digital picture of the same area of the dish was taken at pre-determined time intervals over three days.

*Phospho-erk Western Blot:* HFFs were grown to 100% confluency in 10% FBS DMEM in 100 mm cell culture plates. After the cells had reached 100% confluency, they were washed two times with PBS to remove any traces of serum. Fresh serum free DMEM was added to each plate to induce cellular quiescence. Following the twenty-four hours of serum deprivation, 10 mls of fresh serum free DMEM with sterile PBS 0.1% BSA vehicle or freshly prepared Nle<sup>1</sup>-AngIV in sterile PBS with 0.1% BSA was added to the cells for 10 minutes. Each treatment was performed individually to minimize the variation in phospho-ERK induction due to unequal incubation times. Immediately following the treatment, the cells were washed two times with ice-cold sterile PBS and put on ice. 500  $\mu$ l of ice-cold RIPA buffer with protease and phosphatase inhibitors was added to the dish to lyse the cells. The cells were scraped off of the dish using a rubber policeman. The cell lysate was transferred to 1.5 ml eppendorf tubes and agitated for 15 minutes at 4 degrees Celsius to promote cell lysis. The lysates were clarified by centrifugation at 14,000g for 15 minutes at 4 degrees Celsius. The clarified cell lysate was stored at -80 degrees Celsius.

The cell lysate was thawed on ice and a reducing Laemmli buffer was added to each sample. The samples were boiled for five minutes at 95 degrees Celsius. 20  $\mu$ l of sample was added to each lane of a 10% Tris-HCl gel (Bio-Rad Laboratories, Hercules, CA). The proteins were separated by gel electrophoresis at 120 volts until the dye front ran off of the gel and the proteins were transferred

to nitrocellulose for 40 minutes at 100 volts. After blocking the membrane in Tris-buffered saline with 5% milk for one hour at room temperature, mouse anti-human phospho-erk antibody (Cell Signaling, Danvers, MA) was added at a final concentration of 1:1000 and the primary antibody was incubated overnight at 4 degrees Celsius with gentle agitation. The membranes were washed three times for five minutes each with Tris-buffered saline with 0.05% tween (TTBS) followed by incubation with the secondary horse-radish peroxidase conjugated goat anti-mouse antibody (Pierce, Rockford, IL) for one hour at room temperature in the blocking buffer. Following the secondary antibody incubation, the membranes were washed for three times for five minutes with TTBS and the bands were detected by chemiluminescence.

*Gelatinase Zymography:* MMP-2 activity was detected using gelatin zymography. HFFs were grown in 100 mm plates in 10% FBS DMEM. The cells were serum deprived for twenty-four hours to induce quiescence. The PBS vehicle or Nle<sup>1</sup>-AngIV was added to the cells for three hours. After the treatment, the media was harvested and frozen at -80 degrees Celsius.

Non-reducing Laemmli loading buffer was added to the media samples. 20  $\mu$ l of sample was loaded into each lane of a 10% gelatin gel (Bio-Rad, Hercules, CA) and the proteins were separated by electrophoresis at 120 volts. The enzymes were renatured with a 30 minute wash in 2.5% Triton X-100. The gel was incubated in development buffer (50 mM Tris-HCl, pH 7.5, 200 mM NaCl, 5 mM CaCl<sub>2</sub>, 0.02% Brij-35) at 37 degrees Celsius for 24 hours followed by staining for one hour with 0.1% Coomassie blue in methanol:H<sub>2</sub>O (1:1) solution.

The gels were destained with 45% methanol and 3% acetic acid solution for 30 minutes to reveal zones of lysis created by MMP activity and fixed for one hour in a 0.3% glycerol, 1% glacial acetic acid solution. Digital images of the gels were taken on a light box.

*Animal Use and Care:* All animal experiments were performed under protocol #3534 approved by the Washington State University Institutional Animal Care and Use Committee. Animals were housed two per cage with access to food and water *ad libitum*. During the experiments, the animals were housed one per cage with free access to food and water. Animals were sacrificed by administering an intraperitoneal (IP) injection of 0.1 mg/kg of equithesin followed by cervical dislocation.

*Excisional Wound Healing:* Male Sprague-Dawley rats that were approximately three months old and weighing 400-500 grams were anesthetized with an intramuscular mixture of 1 mg/kg of ketamine/rompun. Their backs were shaved and a depilatory agent (Nair) was applied to remove the hair stubble. The area to be wounded was sterilized with 70% ethanol followed by 0.1% Betadine solution. To create the excision, 1 mm of skin through the panniculus carnosus was excised. For the subcutaneous administration, slow release elvax pellets loaded with Nle<sup>1</sup>-AngIV or vehicle were placed in the wound. The estimated rate of release was approximately 100 µg/kg/day. For systemic administration, 100 µg/kg/day of Nle<sup>1</sup>-AngIV or PBS vehicle was injected IP everyday for the duration of wound healing. The wounds were covered with a bandage for 48 hours, which was secured with Vetrap (3M). At 0,2,4,7,13,15,

and 17 days, the two longest diameters of the wound were measured with digital calipers. Wound area was calculated with the following equation: (Wound Diameter 1 /2)\*(Wound Diameter 2 /2) \*3.14. Wound area at a given time point was divided into the original wound area to calculate the percentage of original wound area.

*Incisional Wound Healing:* Male Sprague-Dawley rats were sedated with ketamine/rompum. Their backs were shaved, a depilatory agent (Nair) was applied to remove hair stubble, and the dorsum was sterilized with 70% ethanol and 0.1% Betadine solution. Two 2 cm incisional wounds were created with surgical scissors and closed with a single suture. 100 µg/kg/day of Nle<sup>1</sup>-AngIV or the vehicle was delivered by daily IP administration. After 7, 10, and 14 days of wound healing, the animals were sacrificed and a 2 inch x 2 inch section of wound containing the healed incision in the center was removed from the dorsum of the rat. The peak breaking strength of the incisional wound was determined with a tensiometer with a constant load of 600 grams/minute. The time of scab release was monitored during these experiments as well.

*Incisional Wound Histology:* The incisions and treatments were performed according to the previously described incisional wound healing protocol. At ten days post-op, the rats were sacrificed by cervical dislocation and the incisions were excised and post-fixed in 10% buffered formalin for 48 hours. The incisions were embedded in paraffin and sectioned at 5 µm. The sections were stained with Masson's Trichrome stain (IMEB Inc., San Marcos, CA) to reveal the collagen fibers in the dermal tissue.



*Obesity-induced Incisional Wound Dehiscence:* C57BLJ lean and leptin-deficient  $ob^{Lep}/ob^{Lep}$  were purchased from Harlan Sprague-Dawley, Inc. (Indianapolis, IN). The mice were sedated with ketamine/rompun. Their backs were shaved and Nair was applied to remove any remaining hair. The surgical area was sterilized with 70% ethanol and 0.1% Betadine solution. Three equidistant one-centimeter wounds were created with sterile surgical scissors on the dorsum of the mouse and closed with Dermabond (Medbrands, Cary, IL). The animals were administered daily IP injections of 100  $\mu\text{g}/\text{kg}/\text{day}$   $\text{Nle}^1\text{-AngIV}$  prepared fresh in sterile PBS with 1% BSA. Control animals received daily IP injections of vehicle only. An observer blinded to the treatments determined the area of wound dehiscence with digital calipers on the seventh and fourteenth postoperative day.

*Statistical Analysis:* Experiments with three groups or more were analyzed with one-way ANOVA followed by Tukey's post-hoc analysis. Experiments with time as an independent variable were analyzed with repeated measures ANOVA with the Student Newman-Keuls post-hoc analysis. Experiments comparing two groups were analyzed with the unpaired student's t-test. Data is presented as mean  $\pm$  SEM with  $p \leq 0.05$  considered statistically significant.

## **Results**

*$\text{Nle}^1\text{-AngIV}$  stimulates dermal fibroblast proliferation, migration, and wound healing in vitro.* The process of reepithelization is made easier by wound

contraction, which brings the wound margins closer together. During the first phase of wound healing, resident dermal fibroblasts in the wound proliferate, and within three days following injury begin migrating into the wound tissue where they deposit a collagen and fibronectin-rich matrix.<sup>9</sup> The dermal fibroblasts undergo a phenotypic change to become differentiated  $\alpha$ -smooth muscle actin expressing myofibroblasts, which are responsible for the force generation during wound contraction. The mechanical tension exerted by the myofibroblasts on the ECM results in the shrinkage of the granulation tissue thereby accelerating wound closure.<sup>10</sup>

Using human dermal fibroblasts as a cell culture model, Nle<sup>1</sup>-AngIV was tested for its ability to activate the basic cellular processes necessary for healing the dermis. As shown in figure 1a and b, Nle<sup>1</sup>-AngIV stimulates fibroblast proliferation and migration at picomolar concentrations. Using the scratch wound assay in which a confluent layer of cells is wounded with a pipet tip, Nle<sup>1</sup>-AngIV accelerates fibroblast wound healing *in vitro* (Figure 1c).

*Nle<sup>1</sup>-AT<sub>4</sub> treatment stimulates phospho-ERK induction in dermal fibroblasts.* To explore the molecular mechanism by which Nle<sup>1</sup>-AngIV is driving fibroblast function, western blotting assays for ERK activation were employed. ERK is phosphorylated downstream of growth factor receptor stimulation, which upon phosphorylation activates transcription factors, such as c-fos, that promote cell proliferation and migration.<sup>11</sup> ERK is activated in fibroblasts seeded in collagen gels in the collagen gel contraction assay, an *in vitro* model for fibroblast mediated wound contraction. Inhibition of ERK with the Mek/ERK inhibitor,

PD98059, inhibits epidermal growth factor (EGF) mediated fibroblast collagen contraction. Additionally, transfection of fibroblasts with ERK silencing RNA inhibits EGF mediated collagen gel contraction.<sup>12</sup>

Human foreskin fibroblasts were grown to confluency and stimulated for ten minutes with picomolar concentrations of Nle<sup>1</sup>-AngIV. Nle<sup>1</sup>-AngIV stimulated an approximate two-fold increase in phospho-ERK expression as compared to vehicle treated controls (Figure 2).

*Nle<sup>1</sup>-AngIV inhibits excisional wound dehiscence.* After it was determined that Nle<sup>1</sup>-AngIV stimulates fibroblast behavior that is consistent with facilitating dermal repair, it was tested in an excisional wound healing model. Excisional wounds are considered to be a traumatic model of wound repair and are characterized by a significant level of wound contraction.<sup>13</sup> The preparation of an excisional wound in a rodent involves removing the epithelial, dermal, and subdermal tissue through the panniculus carnosus. Wound contraction, driven by the newly formed dermal and subdermal connective tissue facilitates wound closure.

1cm<sup>2</sup> excisions were prepared on the backs of rats and wound closure was determined by measuring the area of open wound. During the first week of healing, the control subjects demonstrated a dehiscence of the excisional wound owing to the lag phase of wound healing. Conversely, the Nle<sup>1</sup>-AngIV treatment inhibited excisional wound dehiscence (Figure 3). Additionally, a similar result was observed when this experiment was repeated with daily IP injections of 100 µg/kg/day of Nle<sup>1</sup>-AngIV (unpublished observations).

*Nle<sup>1</sup>-AngIV treatment increases the breaking strength of incisional wounds and causes early scab release.* More than 46 million operations are performed each year in the United States. Shortening the time required for incision wound healing is not only relevant to reducing convalescence, but is also cost-effective. A critical outcome of the wound repair process is restoration of the mechanical properties of tissue strength. The measurement of wound strength provides a quantifiable degree of efficacy to the wound healing process. If sufficient wound strength is not attained, the net effect is wound failure, which is often seen in obese patients suffering from abdominal wound dehiscence. The result is post-operative pain and an increased risk to infection.

The inhibition of dehiscence that was observed in the Nle<sup>1</sup>-AngIV treated excisions may be due to an increase in the adhesive strength of the underlying dermis. To test the effect of Nle<sup>1</sup>-AngIV treatment on wound strength, 2 cm incisions were prepared on the backs of rats and Nle<sup>1</sup>-AngIV was administered by daily IP injections. Wounds were harvested for breaking strength analysis on days 7, 10, and 14. Nle<sup>1</sup>-AngIV treatment resulted in a significant increase in the breaking strength of the incisions on days 7 and 10 (Figure 4a).

The scabs that formed on the incisions were monitored for release during these experiments as well. Previous studies with leptin treated ob<sup>Lep</sup>/ob<sup>Lep</sup> mice demonstrated early scab release due to early wound closure.<sup>14</sup> In the incision wound healing studies, we observed an early release of the scabs in the Nle<sup>1</sup>-AngIV treated rats (Figure 4b).

*Nle<sup>1</sup>-AngIV treatment accelerates dermal tissue healing in incisional wounds.* An increased breaking strength is attributed to an increase in wound ECM deposition. The ECM increases wound thickness and adhesiveness, thereby increasing wound strength. This has been shown most notably with the TGF- $\beta$  family of pro-fibrotic cytokines, which demonstrate a correlative increase in dermal collagen deposition and wound strength.<sup>15</sup>

Using histological cross-sections of the incisions stained with Masson's Trichrome to reveal collagen protein, dermal tissue infiltration and collagen deposition were evaluated in the incisions of the control and Nle<sup>1</sup>-AngIV treated rats at ten days of wound healing, the time point that showed the highest absolute breaking strength induced by Nle<sup>1</sup>-AngIV treatment. Our results reveal that Nle<sup>1</sup>-AngIV treatment expedites dermal invasion into the wound (Figure 5).

*Nle<sup>1</sup>-AngIV treatment results in a decrease in the area of obesity-induced incisional wound dehiscence.* Wound dehiscence, or the separation of the edges of a surgical incision, occurs approximately 7 days postoperatively. The wound may be partially or completely dehisced with or without evisceration. The patient populations that are at the highest risk for wound dehiscence are the elderly, patients on steroids to reduce inflammation, diabetics, and obese patients.<sup>16</sup> Obesity increases the risk of postoperative complications of the skin and underlying tissue, including infection, pressure ulcers, and dehiscence.<sup>17</sup> The current therapy for wound dehiscence is negative pressure wound therapy (NPWT) in which a vacuum is attached to the wound to facilitate wound closure. NPWT is impractical because the patient has to remain immobile for long periods

of time, and painful due to the negative pressure exerted on the open wound. For most patients NPWT is ineffective and surgical closure of the wound is necessary.

Given the effects observed with Nle<sup>1</sup>-AngIV in the wound strength model and histology study, we hypothesized that it would decrease obesity-induced surgical wound dehiscence, a clinically relevant model of impaired wound healing. The ob<sup>Lep</sup>/ob<sup>Lep</sup> mouse model, which has a homozygous deletion of the feeding satiation hormone leptin and develops morbid obesity and type 2 diabetes, was employed in this study. Incisions were created on the dorsum of the ob<sup>Lep</sup>/ob<sup>Lep</sup> mice and closed with Dermabond. Starting on the day of surgery, the mice were administered daily IP injections of 100 µg/kg/day of Nle<sup>1</sup>-AngIV. On the seventh and fourteenth postoperative days, an observer blinded to the treatments determined the area of wound dehiscence with digital calipers. As expected, the wounds of the lean mice did not dehisce and were fully closed one week following surgery. 100% of the wounds in the control and treated obese mice had dehisced by day 7. However, the systemic administration of 100 µg/kg/day of Nle<sup>1</sup>-AngIV reduced the area of wound opening in the ob/ob mice by approximately 50% at day 7 and reduced the incidence of dehiscence at day 14 (Figure 6).

*Nle<sup>1</sup>-AngIV decreases MMP-2 activity.* The balance between ECM deposition and degradation is finely tuned for the proper healing of incisional wounds. Matrix metalloproteinases (MMPs) are a family of zinc and calcium dependent proteases with the major function of degrading the ECM. Since ECM

degradation is the predominant function of MMPs, it is thought that inhibiting MMP activity increases the net ECM deposition in the wound. This increased ECM in the wound acts as a stress-shield for the cells increasing wound strength and inhibiting wound dehiscence.<sup>10</sup>

The effect of Nle<sup>1</sup>-AngIV treatment on excisional and incisional wound healing may be due to the modulation of MMP activity in the wounded dermis. To test this, dermal fibroblasts were treated for 3 hours with one picomolar of Nle<sup>1</sup>-AngIV and MMP-2 activity was detected by gelatin zymography. As shown in figure 6, Nle<sup>1</sup>-AngIV attenuated MMP-2 activity in fibroblasts. These results agree with previous data from our laboratory showing that Nle<sup>1</sup>-AngIV decreases gelatinase expression in cardiac fibroblasts with a correlative increase in collagen deposition (unpublished observations).

## **Discussion**

The results of this study indicate that the AT<sub>4</sub> receptor ligand, Nle<sup>1</sup>-AngIV, stimulates fibroblast responses that are consistent with accelerating wound healing. In addition, we present data indicating that this peptide inhibits excisional wound dehiscence, increases the breaking strength of incisional wounds, and decreases the area of dehiscence in obese mice. Thus, Nle<sup>1</sup>-AngIV treatment may represent a therapeutically important intervention for patient populations that are at an increased risk of wound failure.

In this study, data is presented showing that the acceleration of wound healing is due to the stimulation of fibroblast repair. The *in vitro* data indicates

that Nle<sup>1</sup>-AngIV stimulates fibroblast behavior required for connective tissue healing. In this study, the effects of this peptide on wound angiogenesis and reepithelialization were not examined. We anticipate that angiogenesis and reepithelialization will be stimulated by Nle<sup>1</sup>-AngIV as previous data from our laboratory demonstrates that Nle<sup>1</sup>-AngIV binds with high affinity to both cell types and induces the proliferation of endothelial cells.<sup>17</sup> We are currently conducting experiments to determine if Nle<sup>1</sup>-AngIV is pro-angiogenic and promotes wound reepithelialization.

Several cellular processes contribute to the mechanism of dermal repair. Previous studies have demonstrated that the myofibroblast is the critical cell type required for healing the wounded dermis.<sup>10</sup> However, studies in which the granulation tissue was removed on a daily basis during wound healing have demonstrated that the central granulation tissue, which contains the myofibroblasts, is not the principle contributor to dermal healing.<sup>19</sup> Instead, it was proposed that a newly formed subdermal layer of fibroblasts that connects the dermal tissue to the underlying fascia is responsible for wound closure. The induction of migration in the proliferative subdermal fibroblasts present in the wound margins draws the wound edges together.<sup>20</sup> We favor this mechanism of dermal repair because Nle<sup>1</sup>-AngIV inhibited excisional wound dehiscence as early as two days post-wounding, which precedes the infiltration of wound myofibroblasts. In addition, the inhibition of wound dehiscence and increase in wound strength suggests that Nle<sup>1</sup>-AngIV may accelerate the formation of this tissue and its adherence to the underlying fascia.



With the obesity rate rising in the United States, the impediments to postoperative surgical healing in obese patients are of increasing importance to clinical practitioners. The morbidity rate due to surgical wound dehiscence is estimated to be between 14-50%.<sup>21</sup> Obese patients are at an increased risk of dehiscence of the surgical incision because of impairments in the normal wound healing process and an increased mechanical stress on the edges of the incision. Surgeons often observe dehiscence of abdominal incisions, intestinal incisions, and colonic incisions with evisceration in obese patients. The current treatments for dehiscence are impractical and ineffective, usually requiring additional surgeries to close the wound. Currently, no treatment modalities exist for preventing incisional wound dehiscence in these patients. Of great clinical relevance in this study is Nle<sup>1</sup>-AngIV reduction of the area of dehiscence in obese mice. Ligands that target the AT<sub>4</sub> receptor may be the first in class for treating this condition.

Fibroblast adherence to the ECM has been demonstrated to be a critical regulator of early wound healing. Remodeling of the ECM by MMPs repairs the dermal tissue by modulating the processes of cell proliferation, migration, and adhesion. It has been reported that MMP inhibitors increase the breaking strength of incisional wounds, intestinal anastomoses, and colonic anastomoses.<sup>22,23</sup> Additionally, excessive MMP activity has been detected in chronic wounds, resulting in tissue destruction and delayed wound closure.<sup>24</sup> In this study, acute treatment with Nle<sup>1</sup>-AngIV decreased MMP-2 activity in dermal fibroblasts. Therefore, it is probable that Nle<sup>1</sup>-AngIV mechanism for inhibiting

dehiscence and increasing wound strength is via the regulation of MMP activity. Future studies aimed at determining Nle<sup>1</sup>-AngIV effect on MMPs in the wound is underway in our laboratory.

Wound healing continues to be a formidable challenge for clinical practitioners worldwide. Currently, Regranex (recombinant platelet-derived growth factor) is the only available treatment for chronic wounds. It is expensive to produce and has limited clinical utility. We propose that a new family of small molecules that have high affinity for the AT<sub>4</sub> receptor have usefulness in accelerating wound healing. Additionally, these molecules are relatively inexpensive and simple to produce. Further research aimed at characterizing alternative ligands with improved stability characteristics and alternative administration routes are currently under investigation in our laboratory.

### **Acknowledgements**

Pacific Northwest Biotechnology, LLC, funded this study.

## References

1. Wright JW, Krebs LT, Stobb JW, Harding JW. The Angiotensin IV System: Functional Implications. *Frontiers in Neuroendocrinology* 1995;16: 23-52.
2. Viswanathan M, Saavedra JM. Expression of angiotensin II AT2 receptors in the rat skin during experimental wound healing. *Peptides* 1992;4:783-6
3. Kou B, Vatish M, Singer D. Effects of Angiotensin II on human endothelial cells survival signaling pathways and its angiogenic response. *Vascul Pharmacol* 2007;47:199-208.
4. Munk VC, Miguel LS, Petimpol M, Butz N, Banfi A, Eriksson U, Hen L, Humar R, and Battegay EJ. Angiotensin II Induces Angiogenesis in the Hypoxic Adult Mouse Heart In Vitro Through an AT 2-B2 Receptor Pathway. *Hypertension* 2007;49:1178-85.
5. Rodgers K, Xiong S, Felix J, Roda N, Espinoza T, Maldonado S, Dizerega G. Development of angiotensin (1-7) as an agent to accelerate dermal repair. *Wound Rep Regen* 2001;9:238-247.
6. Clark MA, Gonzalez N. Angiotensin II stimulates astrocyte mitogen-activated protein kinase activity and growth through EGF and PDGF receptor transactivation. *Regul Pept* 2007;144:115-22.
7. Brilla CG, Zhou G, Matsurbara L, Weber KT. Collagen Metabolism in cultured rat cardiac fibroblasts: response to angiotensin II and aldosterone. *J. Mol Cell Cardiol* 1994;7:809-20.

8. Rodgers KE, Ellefson DD, Espinoza T, Roda N, Maldonado S, Dizerega GS. Effect of NorLeu<sup>3</sup>-A(1-7) on scar formation over time after full-thickness incision injury in the rat. *Wound Rep Regen* 2005;13:309-17.
9. Martin, P. Wound Healing-Aiming for Perfect Skin Regeneration. *Science* 1997;4:75-80.
10. Tomasek JJ, Gabbiani G, Hinz B, Chaponnier C, Brown RA. Myofibroblasts and Mechanoregulation of Connective Tissue Remodelling. *Nature Reviews* 2002;3:349-363.
11. Lee DJ, Rosenfeldt H, Grinnell F. Activation of ERK and p38 MAP Kinases in Human Fibroblasts during Collagen Matrix Contraction. *Exp Cell Res* 2000;257:190-197.
12. Smith KD, Wells A, Lauffenburger DA. Multiple signaling pathways mediate compaction of collagen matrices by EGF-stimulated fibroblasts. *Exp Cell Res* 2006;312:1970-1982.
13. DiPietro LA and Burns AL. *Wound Healing Methods and Protocols*. Totowa: Human Press, 2003.
14. Goren I, Kampf H, Podda M, Pfeilschifter J, Frank S. Leptin and wound inflammation in diabetic ob/ob mice. *Diabetes* 2003; 52: 2821-2832.
15. Cromack DT, Porras-Reyes B, Purdy JA, Pierce GF, Mustoe TA. Acceleration of tissue repair by transforming growth factor beta 1: identification of in vivo mechanism of action with radiotherapy-induced specific healing deficits. *Surgery* 1993; 113:36-42.

16. Hunter S, Thompson P, Langemo D, Hanson D, and Anderson J. Understanding wound dehiscence. *Nursing* 2007;37: 28-30.
17. Baugh N. Wound Wise: Wounds in Surgical Patients Who Are Obese. *Am J Nurs* 2007;6: 40-50.
18. Hall KL, Venkateswaran S, Hanesworth JM, Schelling ME, Harding JW. Characterization of a functional angiotensin IV receptor on coronary microvascular endothelial cells. *Reg Peptides* 1995;58:107-115.
19. Gross J, Farinelli W, Sadow P, Anderson R, Bruns R. On the mechanism of skin wound "contraction": A granulation tissue "knockout" with a normal phenotype. *Proc Natl Acad Sci USA* 1995;92:5982-5986.
20. Watts GT, Grillo HC, Gross J. Studies in Wound Healing:II. The Role of Granulation Tissue in Contraction. *Ann Surg* 1958;2:153-160.
21. Hahler B. Surgical wound dehiscence. *Medsurg Nurs* 2006;5:296-300.
22. Bullard KM, Lund L, Mudgett JS, Mellin TN, Hunt TK, Murphy B, Ronan J, Werb Z, Banda MJ. Impaired Wound Contraction in Stromelysin-1-Deficient Mice. *Ann Surg* 1999;2:260-265.
23. de Hingh IHJT, Siemonsma MA, de Man BM, Lomme RMLM, Hendriks T. The matrix metalloproteinase inhibitor BB-94 improves the strength of intestinal anastomoses in the rat. *Int J Colorectal Dis* 2002;17:348-354.
24. Witte MB, Thornton FJ, Kiyama T, Efron DT, Schulz GS, Moldawer LL, Barbul A. Metalloproteinase inhibitors and wound healing: a novel enhancer of wound strength. *Surgery* 1998;2:464-70.

25. Medina A, Scott PG, Ghahary A, Tredget EE. Pathophysiology of Chronic Nonhealing Wounds. *J Burn Care Rehabil* 2005;4:306-319.

### **Figure Legends**

#### **Figure 7. Nle<sup>1</sup>-AngIV Stimulates HFF Proliferation, Migration, and Wound Healing.**

**A.** HFFs (5000/well) were treated with the indicated concentrations of Nle<sup>1</sup>-AngIV for 24 hours. After 24 hours of proliferation, WST-8 dye was added to the cells and incubated for one hour at thirty-seven degrees Celsius. The absorbance of reduced WST-8 dye was quantitated on a Biotek plate reader at 440 nm. N=6, mean +/- SEM **B.** 50,000 HFFs were seeded into the top chamber of Falcon transwell inserts and allowed to attach for two hours at thirty-seven degrees Celsius. Media containing either Nle<sup>1</sup>-AngIV or PBS was added to the bottom chamber. The same concentration of Nle<sup>1</sup>-AngIV or PBS was added to the top chamber. The cells migrated for four hours after which they were fixed and stained. Cells that had migrated to the underside of the insert were counted in four random fields at 40x. N=4, mean +/- SEM **C.** HFFs were grown to 100% confluency in Integrid Petri dishes. The monolayer was scraped with a pipet tip and Nle<sup>1</sup>-AngIV or PBS was added to the media. The HFFs were allowed to invade the denuded area over three days and pictures were taken each day at the same location of the plate with a light microscope. \* indicates p<0.05 vs. control by Tukey's post-hoc analysis.

**Figure 8. Nle<sup>1</sup>-AngIV Stimulates Phosphorylated-Erk Induction in HFFs.**

HFFs were grown to confluency in 100 mm dishes in normal growth media. Twenty-four hours prior to treatment, the cells were serum deprived to induce quiescence. Following serum deprivation, the cells were stimulated for ten minutes with Nle<sup>1</sup>-AngIV or the PBS vehicle. The cells were lysed in Ripa buffer and proteins were separated by electrophoresis. Phosphorylated Erk expression was normalized to total erk band density. N=2 and has been repeated one time with similar results.

**Figure 9. Nle<sup>1</sup>-AngIV Inhibits Excisional Wound Dehiscence.**

1mm<sup>2</sup> excisional wound was made on the dorsum of male Sprague-Dawley rats under aseptic conditions. Elvax pellets releasing 100 µg/kg/day Nle<sup>1</sup>-AngIV or the 1% BSA PBS vehicle was placed into the wound. N=4, mean +/- SEM. The wound area was determined on postoperative days 2, 4, 7, 10, 13, 15, and 17 with digital calipers. Repeated measures ANOVA indicated a significant effect of treatment with p<0.05 vs. control.

**Figure 10. Systemic Nle<sup>1</sup>-AngIV Treatment causes Early Scab Release and Increases the Breaking Strength of Incisional Wounds.**

**A.** 2 cm incisional wounds were created on the backs of male Sprague-Dawley rats and closed with one suture tied in the center of the wound. 100 µg/kg/day Nle<sup>1</sup>-AngIV or the 1% BSA PBS vehicle was administered by IP injection on a daily basis starting on the day of wounding. At 7, 10, and 14 days of healing, the wounds were harvested and subjected to breaking strength analysis. N=6-8, mean +/- SEM. \* p≤0.05 by the unpaired student's t-test. **B.** During the incisional studies, 100 µg/kg/day of Nle<sup>1</sup>-AT<sub>4</sub> treatment caused an early scab release. N=9, mean +/- SEM. \*p<0.05 vs. control by the unpaired student's t-test.

**Figure 11. Nle<sup>1</sup>-AngIV increases collagen deposition in incisional wounds.**

2 cm incisional wounds were created on the backs of male Sprague-Dawley rats and closed with one suture tied in the center of the wound. 100 µg/kg/day of Nle<sup>1</sup>-AngIV or the 1% BSA PBS vehicle was administered by IP injection on a daily basis starting on the day of wounding. At 10 days of healing, the wounds were harvested for histological analysis with Masson's Trichrome stain to reveal wound collagen deposition.



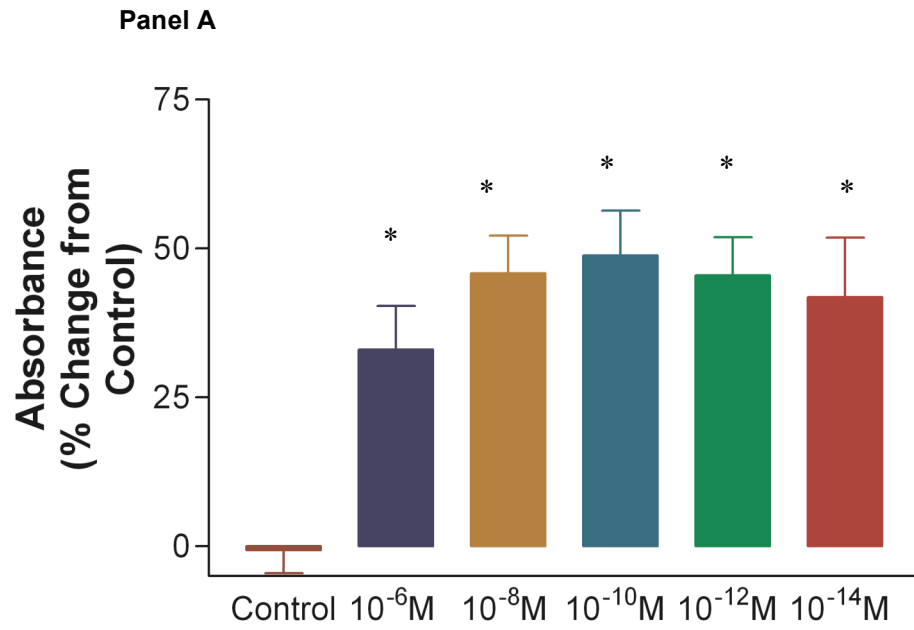
**Figure 12. Systemic Nle<sup>1</sup>-AngIV Treatment Decreases the Area of Incisional Wound Dehiscence in Ob/Ob mice.**

1 cm incisional wounds were created using aseptic conditions on the backs of C57BlJ lean and ob/ob mice. The wounds were closed with dermabond. 100  $\mu\text{g}/\text{kg}/\text{day}$  of Nle<sup>1</sup>-AngIV or the 1% BSA containing PBS vehicle was administered by IP injection everyday. One week following surgery, the dermabond was removed from the wounds and the area of dehiscence was determined with digital calipers by an observer blinded to the treatments. N=6-9, mean  $\pm$  SEM. P=0.02 for a treatment effect by two-way ANOVA. \*p<0.05 vs. control by Student-Newman-Keuls post-hoc analysis.

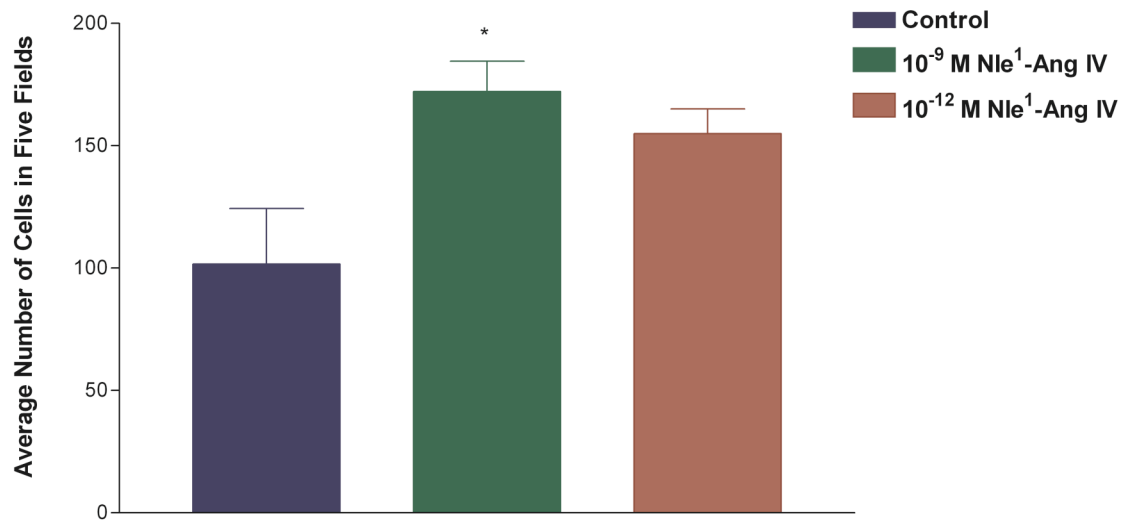
**Figure 13. MMP-2 Activity is reduced by Nle<sup>1</sup>-AngIV treatment.**

Confluent HFFs were stimulated with one picomolar of Nle<sup>1</sup>-AngIV for three hours. The media was harvested and MMP-2 activity was detected using gelatin zymography. N=3, mean  $\pm$  SEM. \*p $\leq$ 0.05 vs. control.

Figure 7.

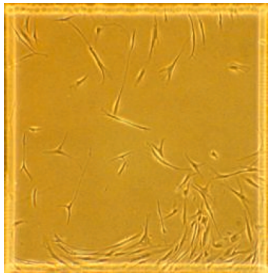
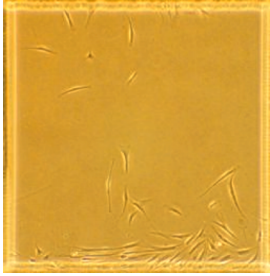
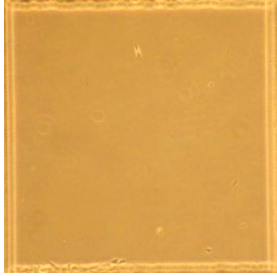


**Panel B**

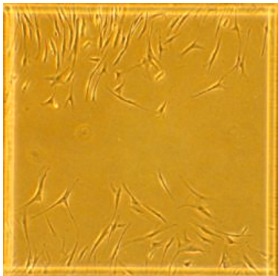


**Panel C**

Control



$10^{-6}$  M Nle<sup>1</sup>-AngIV



Day 1

Day 2

Day 3

**Figure 8.**

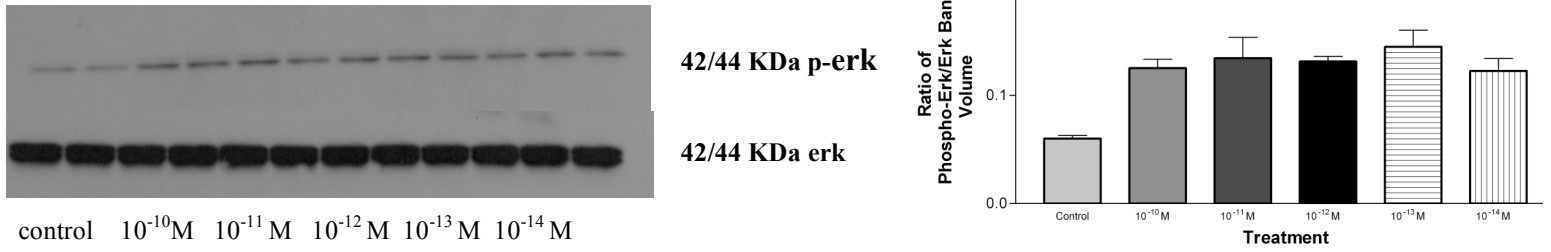


**Figure 9.**

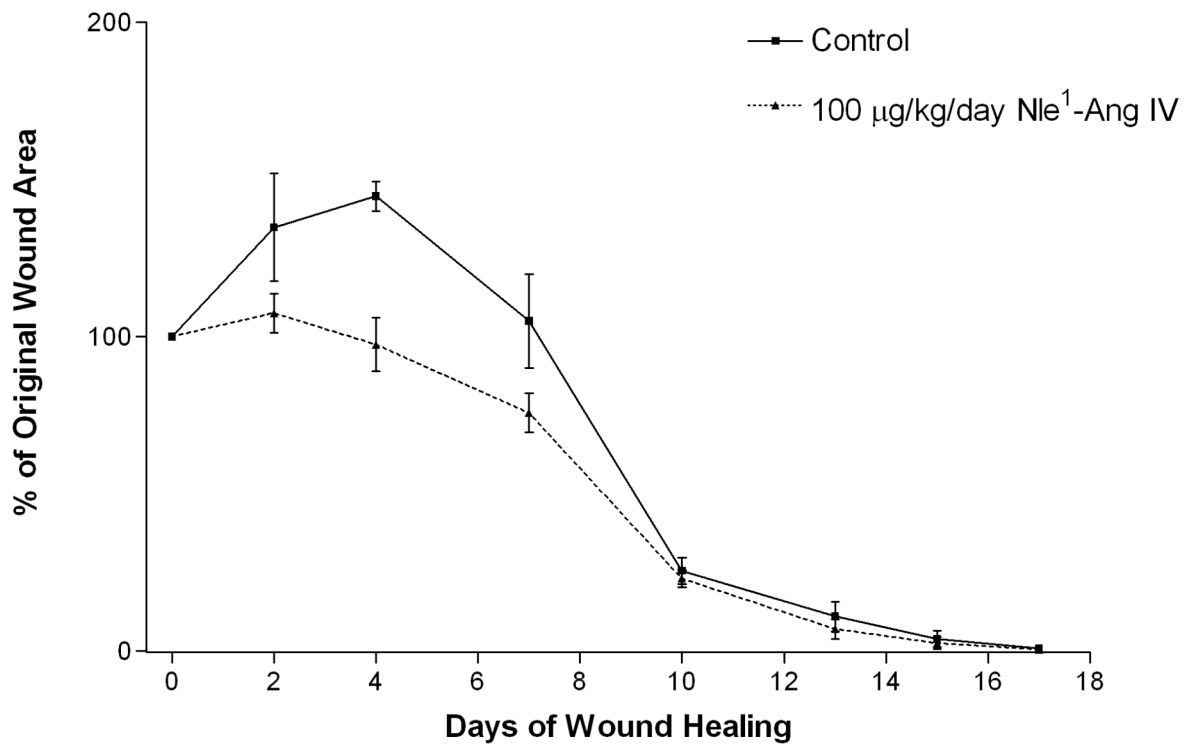
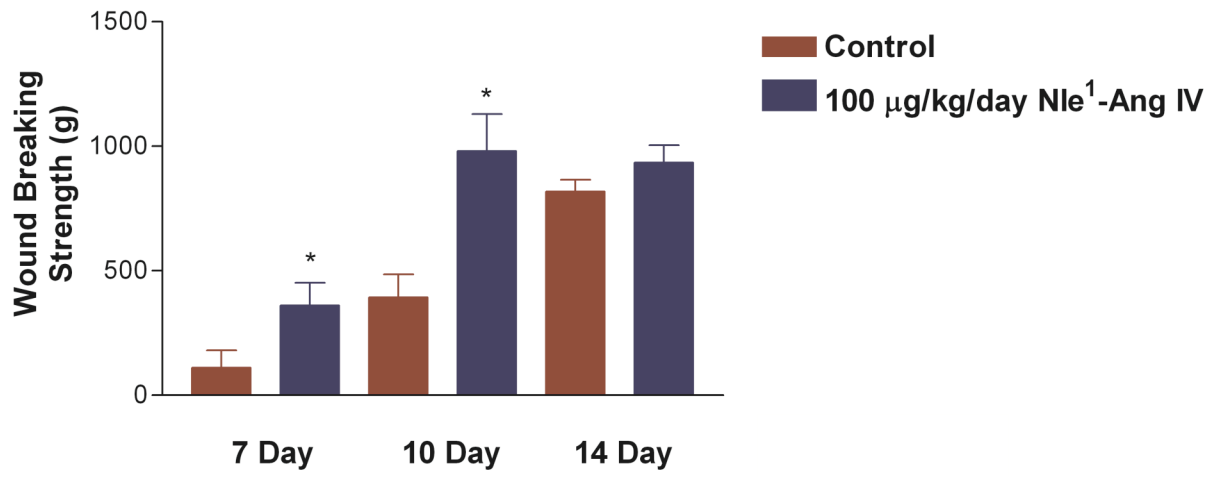


Figure 10.

Panel A



Panel B

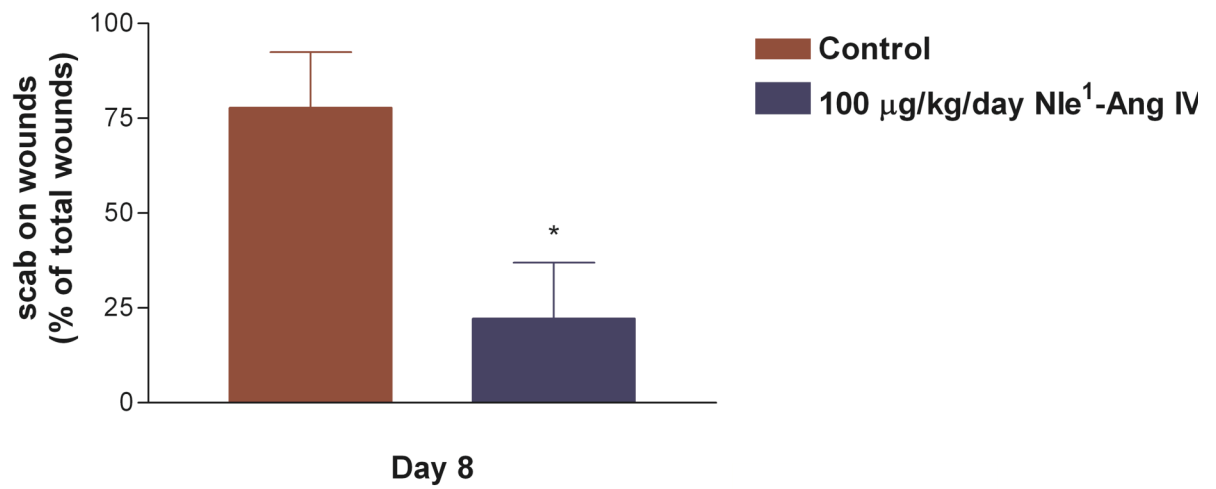
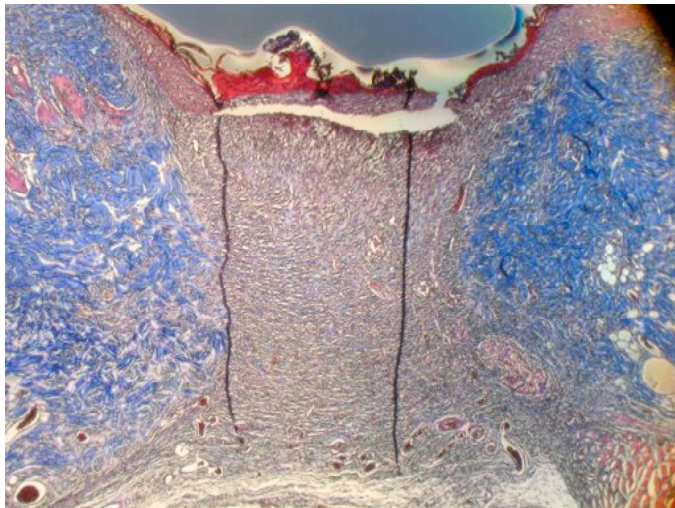


Figure 11.

Day 10

Control



100  $\mu\text{g}/\text{kg}/\text{day}$   
Nle<sup>1</sup>-Ang IV

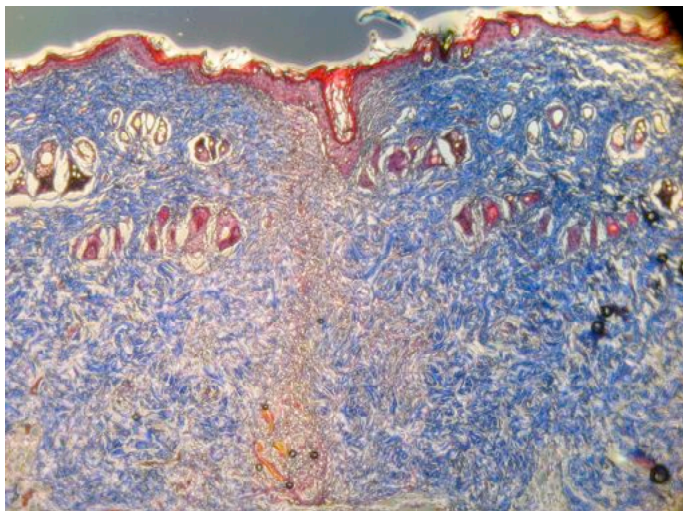


Figure 12.

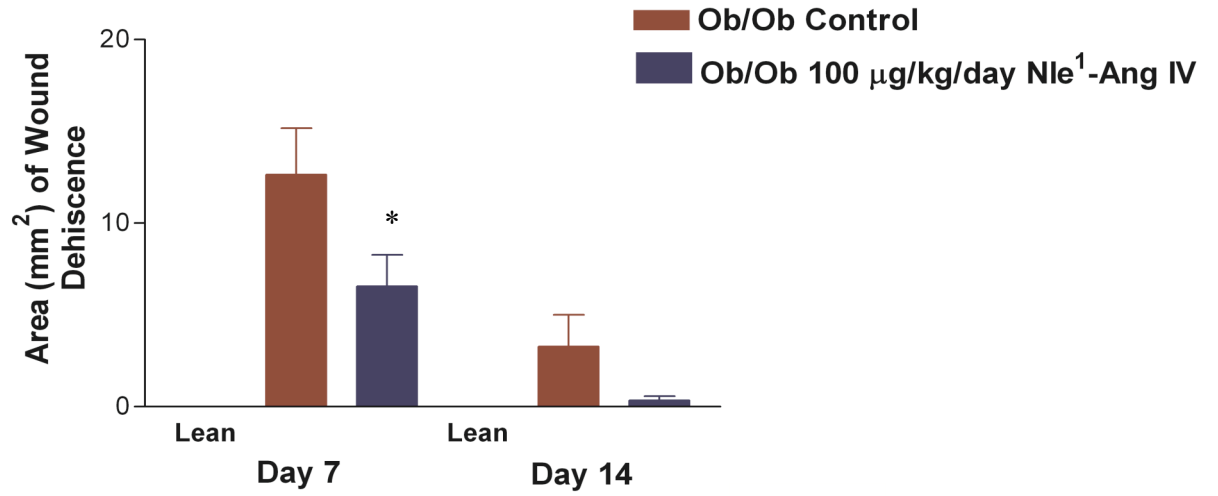
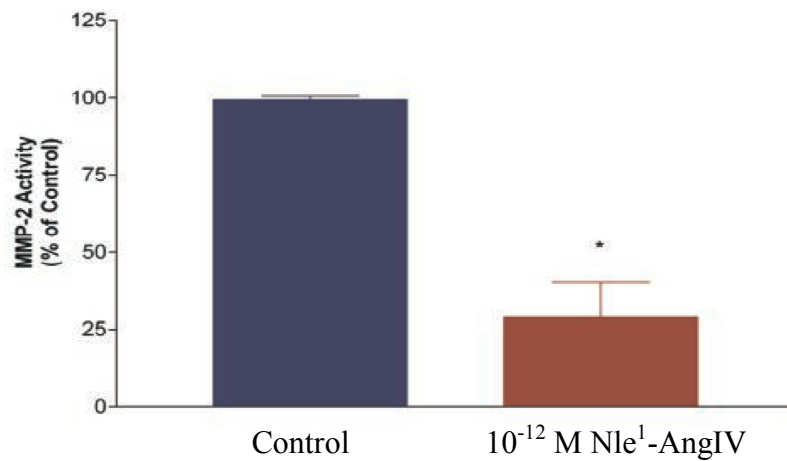
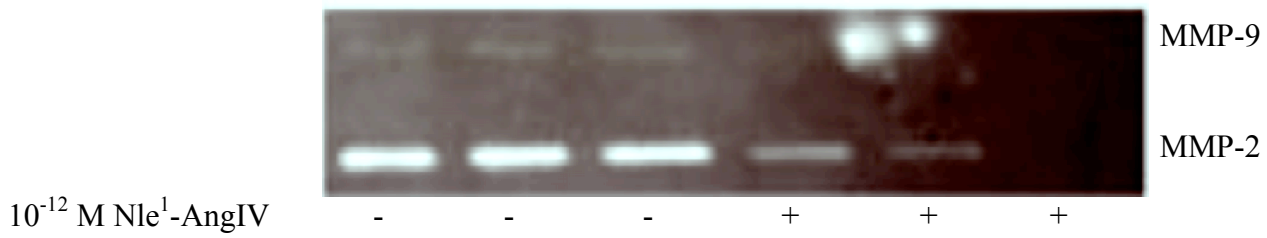


Figure 13.



## Chapter IV

### Conclusion

In this dissertation, our laboratory provides compelling evidence that the AT<sub>4</sub> antagonist, Norleual, disrupts c-Met signaling and cell function and the AT<sub>4</sub> agonist, Nle<sup>1</sup>-Ang IV, accelerates wound healing. Of practical importance is the simplicity and low cost associated with the production of these molecules. Currently, monoclonal antibodies and recombinant proteins are dominating the molecular therapy field. They have proven to be difficult and expensive to produce and alternatives are desperately needed.

Norleual's ability to perturb c-Met signaling and function make it an attractive candidate for a wide array of diseases dependent on c-Met activity, such as cancer, diabetic retinopathy, and malaria infection. Future studies will be aimed at determining Norleual's effect on cell types that harbor aberrant forms of c-Met. Our expectation is that cells which overexpress c-Met will be more sensitive to Norleual treatment than those cell types which have relatively low levels of c-Met expression. Future efforts to continue the development of Norleual as a therapeutic agent include establishing a pharmacokinetic profile and performing GLP toxicology studies. Modifications to Norleual's structure to improve stability characteristics include the addition of Norleucine in the D configuration on the N-terminus to prevent metabolism by aminopeptidases. Additionally, Norleual's effect on receptor systems other than c-Met will be investigated, because binding data indicates that Norleual interacts with multiple sites on the cell membrane.



Future studies to continue the development of Nle<sup>1</sup>-AngIV as a therapeutic agent to accelerate wound healing include formulating Nle<sup>1</sup>-AngIV in hydrogels for topical delivery, which has the direct advantage of delivering the molecule directly to the site and reducing systemic exposure. Nle<sup>1</sup>-Ang IV effect on the time to closure, incidence of complete closure, and the rate of closure during diabetic wound healing will be determined as these are the parameters most relevant to a clinical scenario. Other models of wound healing that may be employed include the steroid-induced wound failure model, incisional hernias, and intestinal anastomoses. A full pharmacokinetic profile and pre-clinical toxicology studies will be required to continue the development of Nle<sup>1</sup>-AngIV as a clinical agent for wound healing. It is expected that Nle<sup>1</sup>-AngIV will be very labile due to its peptide structure. Structural modifications to increase the half-life of the molecule include changing the L-Norleucine to a D configuration on the N-terminus and the insertion of non-peptide links.

Nle<sup>1</sup>-Ang IV and Norleual elicit dramatic effects at picomolar concentrations indicating a high-affinity binding interaction between the ligand and the receptor. The receptor for Norleual has recently been elucidated as the c-Met receptor. However, further work is required to determine the protein responsible for transducing Nle<sup>1</sup>-Ang IV activity. Unpublished observations from our laboratory indicate that Nle<sup>1</sup>-Ang IV may be a c-Met partial agonist as it induces cell replication and motility, but antagonizes HGF/c-Met dependent effects. Further studies using surface plasmon resonance followed by mass spectrometry analysis will shed light on Nle<sup>1</sup>-Ang IV molecular target.

Additionally, we are currently determining the structural requirements needed for Norleual and Nle<sup>1</sup>-Ang IV receptor binding and activity. These include amino acid changes to the N and C terminal domains in addition to the insertion of non-peptide links to improve stability characteristics. Recently, we obtained promising *in vitro* data on a handful of these modified peptides (Figures 1 and 2).

The broad physiological distribution of AT<sub>4</sub> receptors indicates that we have only scratched the surface with regards to the possibility of using these ligands as interventions for disease. Numerous treatment possibilities exist including reversing fibrotic disease and macular degeneration. It is our long-term goal to bring these molecules to market to meet an ever-increasing demand for low-cost, effective treatments.

## Figure Legends

### **Figure 14. Nle<sup>1</sup>-Ang IV, D-Nle<sup>1</sup>-Ang IV, and fragments stimulate dermal fibroblast proliferation.**

5000 dermal fibroblasts were seeded into the wells of a 96-well plate in complete growth medium. The cells were serum starved for 24 hours to induce quiescence before adding the indicated concentrations of peptide prepared fresh in sterile PBS with 0.1% BSA. Controls received the PBS 0.1% BSA vehicle only. The cells were allowed to grow under these conditions for 24 hours before adding 10  $\mu$ l of WST-8 reagent and incubating for one hour at 37°C. The absorbance was quantitated on a plate reader at 440 nm. For consistency, all values represent the percentage change from control. N=6, mean +/- SEM.

### **Figure 15. D-Noreual-6AH and modified peptides attenuate HGF/c-Met mediated cell migration.**

50,000 MDCK cells were labeled with 5  $\mu$ g/ml of Vybrant Dil (Molecular Probes) and seeded into the top chamber of a BD Falcon Fluoroblok cell culture insert (BD Biosciences) in 1% fetal bovine serum (FBS) growth media. The cells were allowed to attach to the membrane for two hours before adding 300  $\mu$ l of 1% FBS growth media containing the indicated concentrations of peptide with 10 ng/ml of HGF to the bottom chamber. An equivalent concentration of peptide was added to the top chamber. The cells were allowed to migrate for 14 hours before analyzing fluorescence on the bottom chamber. N=6, mean +/- SEM. All values represent the percentage of HGF response.

Figure 1.

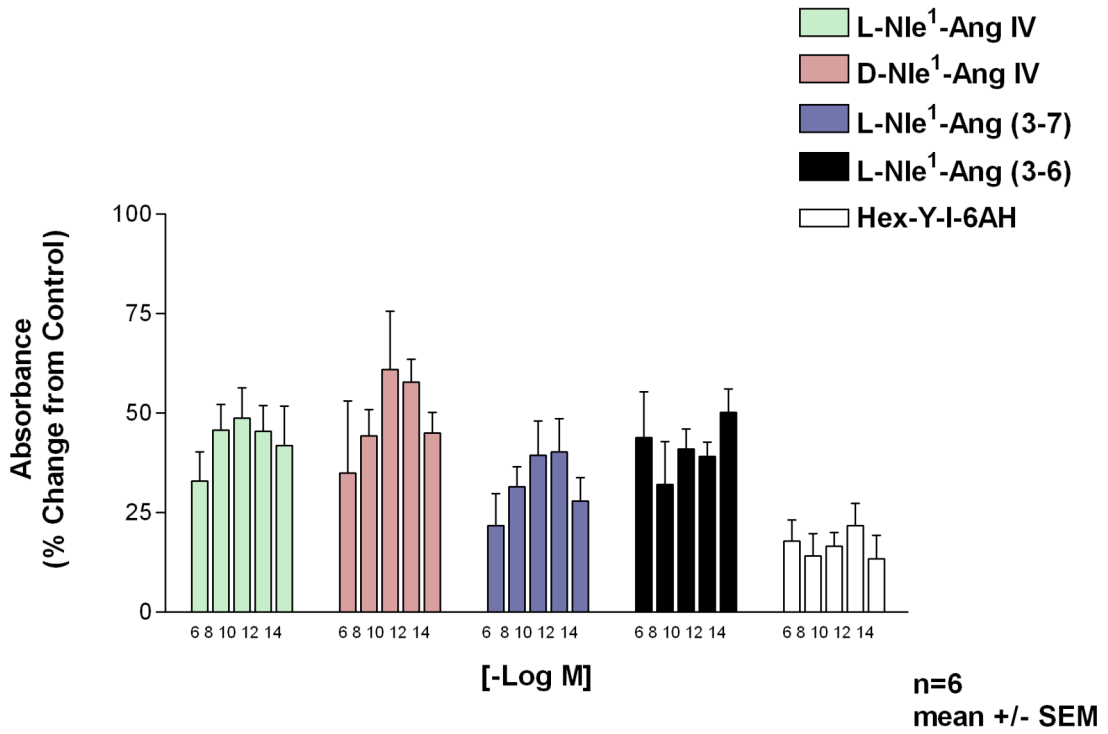


Figure 2.

